1918
TALLINNA TEHNIKAÜLIKOOL
TALLINN UNIVERSITY OF TECHNOLOGY

Faculty of Science
Department of Gene Technology
Chair of Genomics and Proteomics

**Ann Karafin**

# Zn(II) and Cu(II) induced aggregation and fibrillation of Alzheimer's amyloid peptide

**Master Thesis**

Supervisors: **Vello Tõugu, Ph.D.**
Chair of Genomics and Proteomics
Department of Gene Technology
Tallinn University of Technology
**Prof. Peep Palumaa, Ph.D.**
Chair of Genomics and Proteomics
Department of Gene Technology
Tallinn University of Technology

Tallinn 2009

1918
TALLINNA TEHNIKAÜLIKOOL
TALLINN UNIVERSITY OF TECHNOLOGY

Matemaatika-loodusteaduskond
Geenitehnoloogia instituut
Genoomika ja proteoomika õppetool

**Ann Karafin**

# Alzheimeri amüloid-β peptiidi fibrillatsioon ja agregatsioon Zn(II) ja Cu(II) toimel

**Magistritöö**

Juhendajad: Vello Tõugu, Ph.D.
Genoomika ja proteoomika õppetool
Geenitehnoloogia Instituut
Tallinna Tehnikaülikool
Prof. Peep Palumaa, Ph.D.
Genoomika ja proteoomika õppetool
Geenitehnoloogia Instituut
Tallinna Tehnikaülikool

Tallinn 2009

# CONTENTS

# ABBREVIATIONS

| | |
|---|---|
| Aβ | amyloid-β peptide |
| AD | Alzheimer's disease |
| APP | Amyloid precursor protein |
| CQ | Clioquinole |
| EPR | Electron paramagnetic resonance |
| FAD | Familial Alzheimer's disease |
| HEPES | 4-(2-hydroxyethyl)-1-piperazineethanesulfonic acid |
| HFIP | 1,1,1,3,3,3-hexafluoro-2-propanol |
| ICP-MS | Inductively-coupled-plasma mass-spectrometry |
| MALDI TOF MS | Matrix-assisted laser desorption/ionization time-of-flight mass spectrometry |
| MT | Metallothionein |
| NMR | Nuclear magnetic resonance |
| NFT | Neurofibrillary tangles |
| SEC | Size exclusion chromatography |
| ThT | Thioflavin T |
| TEM | Transmission Electron Microscopy |
| TSPP | Tetrakis(4-sulfophenyl)porphine |

# INTRODUCTION

Alzheimer's disease (AD) is a progressive neurodegenerative disorder characterized by an increasing impairment in normal memory and cognitive processes that significantly diminishes a person's daily functioning and ultimately leads to death. AD is the most prevalent cause of dementia in the elderly population and the third leading cause of death in developed countries [1].

One of the key events in AD pathology is the fibrillation and aggregation of amyloid-β (Aβ) peptides into amyloid plaques. Aβ aggregation *in vivo* occurs in the presence of a large variety of biomolecules and ions that may play an essential role in amyloidogenesis. First candidates for the molecules directly affecting the fibrillogenesis *in vivo* are Zn(II) and Cu(II). Amyloid plaques contain elevated levels of transition metal ions [2, 3] whereas copper and iron bound to Aβ are electrochemically active and contribute to oxidative stress. Biometals affect Aβ fibrillation process *in vitro*, but the latter data are often contradictory and not quantitative. However, despite the incomplete knowledge about the effect of metals on amyloidogenesis, a new therapeutic approach called "metal-chelation therapy" has been developed and some metal chelators have already been tested in phase II clinical trials. Unfortunately, only limited therapeutic aspect was observed, which calls for more detailed studies about the role of metal ions and metal chelators on Aβ aggregation and amyloidogenesis.

The aim of the current study was to clarify the effects of zinc and copper and metal chelating agents on the wild type and mutant $A\beta_{42}$ peptide fibrillation. Realization of this task required an elaboration of a fast and reproducible method for carrying out and monitoring the Aβ fibrillation process. A series of experiments was planned to validate the relevance of clinically used metal chelators in the context of metal chelation therapy of AD.

# 1. LITERATURE

## 1.1. Alzheimer's disease

Dementia is defined as progressive damage of cognitive and other higher functions as a result of organic brain disease. The prevalence of dementia in the western world is under 1% among people aged 60-64, but rises with age, reaching 24% to 33% in the 85 and older [4]. In 2001 more than 24 million people had dementia and it will probably double in every twenty years reaching 81 million by 2040. The most frequent cause of dementia in the elderly is Alzheimer's disease (AD) accounting for 60% - 80% of all cases [5].

More than a hundred years ago Alois Alzheimer gave a lecture in Munich describing the disease for the first time. Alzheimer's original patient, a woman referred to as Auguste D., had several symptoms of AD that are observed in most patients: progressive memory impairment, disordered cognitive function, altered behaviour including paranoia, delusions and loss of social appropriateness and a progressive decline in language function [6]. The disease course is insidious and AD patients might live up to 20 years after the initial diagnosis, although the median survival is between five and ten years [7].

Age is the major risk factor for AD with doubling of the risk every five years after the age of 65 [8]. Genetic factors, that play an important role in determining AD risk, are inflammatory genes and apolipoprotein E [9]. Other risk factors include reduced brain reserve, poor education, decreased mental and physical activities, traumatic head injuries, vascular diseases, smoking, obesity and diabetes. The preventive modifiers for AD are anti-inflammatory agents, supportive environment during childhood, high mental and physical activity, antioxidants and lipid lowering agents [10].

Most forms of AD are sporadic (i.e. idiopathic), with the onset of symptoms generally beginning after 65-70 years of age. A small proportion of cases, however, exhibit a Mendelian pattern of inheritance and are referred to as familial Alzheimer's disease (FAD), which usually has an early onset (<65 years of age). Neuropathologically, both FAD and sporadic AD are remarkably similar and are characterized by two hallmark

proteinaceous aggregates: amyloid plaques and neurofibrillary tangles (NFT). In addition to these aggregates the AD brain is also marked by additional neuropathological alterations, including the loss of synapses, atrophy, the selective depletion of neurotransmitter systems and by Lewy bodies in a minority of cases [11-13].

Amyloid plaques, that are extracellular aggregates, are composed mainly of small, 4 kDa β-amyloid (Aβ) peptides, acting as a nidus for the recruitment of astrocytes and microglia and for the deposition of other proteins [14, 15]. Within the amyloid plaques Aβ is organized into insoluble fibrils of 6-10 nm diameters. Plaques are usually found in limbic brain regions, such as the hippocampus and amygdala, and also in specific cortical and subcortical areas [15]. Most plaques are of the diffuse type, containing or surrounded by few dystrophic dendrites and axons in contrast to the less frequent neuritic plaques, in which dystrophic neurites are a prominent and commonplace feature [16].

The second type of aggregates NFTs are intracellular depositions of hyperphosphorylated degenerate filaments, which result from the aggregation of the microtubular protein tau [6]. NFTs are significantly present in the entorhinal cortex and hippocampus as well as in the neocortex in varying but usually prominent concentrations [17].

## 1.2. Amyloid cascade hypothesis

Aβ is a natural product and is present in the brains and cerebrospinal fluid of normal humans throughout life, therefore the presence of Aβ does not cause neurodegeneration [18]. Aβ is in three fractions in the brain: membrane-linked, aggregated and soluble. In healthy individuals most of the Aβ is membrane linked but in people with AD the aggregated and soluble fraction (structures shown on Figure 1) is more prominent [19]. The length of Aβ, 40-42 amino acids, is an important factor in AD pathogenesis: the less prevalent form of the peptide $A\beta_{42}$ is particularly enriched in β-amyloid deposits but in biological fluids there is more $A\beta_{40}$ [20].

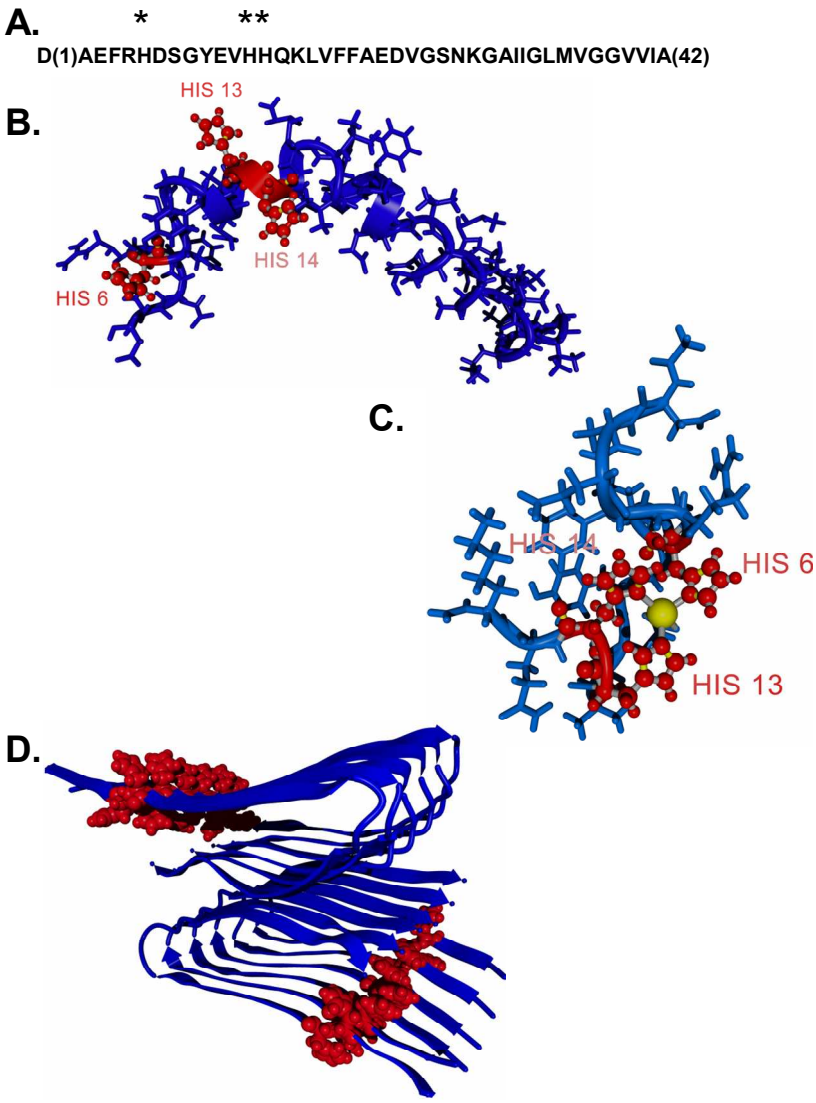


**Figure 1.** The structures of different Aβ conformations. (a) – sequence of human $Aβ_{42}$, histidine residues are indicated by an asterisk (b) α-helix of Aβ [21] (c) the structure of $Aβ_{1-16}$ upon zinc binding [22] (d) Structure of Aβ protofilament. Aβ protofilaments repeating unit consists of two juxtaposed Aβ molecules, which form hydrogen bonds with the adjoining juxtaposed Aβ peptide units and form cross β amyloid core structure of the fibril. Atomic coordinates were kindly provided by Dr. Robert Tycko. Histidine residues are depicted in red, Zn(II) ion in yellow.

The Aβ peptide is derived from amyloid precursor protein (APP) through proteolysis. There are two alternate pathways for APP cleavage: the non-amyloidogenic and the amyloidogenic. In the non-amyloidogenic pathway APP is cleaved by the membrane-associated metalloprotease α-secretase within the Aβ domain (between residues 16 and 17). This prevents the formation of Aβ, and instead results in the release of the large soluble extracellular N-terminal portion of APP (APPsα) and a C-terminal fragment consisting of 83 residues (C83). C83 might undergo further processing by γ-secretase to

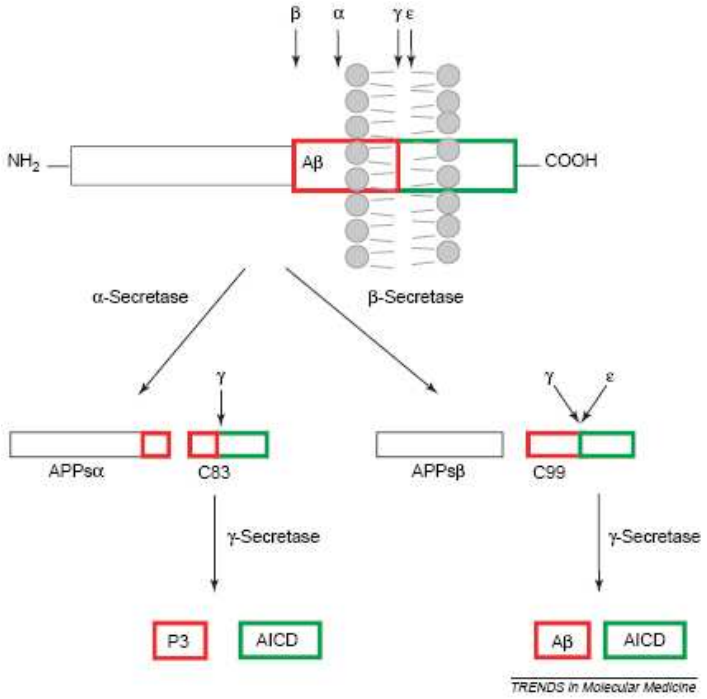


**Figure 2.** APP-processing pathways [16]. Abbreviations: AICD - APP intracellular domain; APPsα - large soluble extracellular N-terminal portion of APP; APPsβ – shorter soluble N-terminus of APP; C83 – C-terminal fragment of APP consisting of 83 residues; C99 – C-terminal fragment of APP consisting of 99 residues.

release the p3 peptide, which is considered non-amyloidogenic, although it is deposited in diffuse plaques. In the amyloidogenic pathway APP undergoes two sequential endoproteolytic steps First the cleavage by β-secretase, the enzyme known as BACE1 (b-site APP-cleaving enzyme), at the N-terminal region of the Aβ sequence. This generates a slightly shorter soluble N-terminus (APPsβ) and the amyloidogenic C-terminal fragment (C99). Then the C99 is cleaved by γ-secretase liberating the C-terminal 50 residues of APP, which is known as APP intracellular domain (AICD) and Aβ [16]. A schematic overview of this pathway is shown on Figure 2.

It has long been argued that the deposition of amyloid is an early step in AD pathogenesis [15]. The amyloid cascade hypothesis of AD, as formalized by Hardy and Higgins in 1992, states that "Aβ precipitates to form amyloid and, in turn, causes neurofibrillary tangles and cell death" [23]. An overview of the mechanism behind amyloid cascade hypothesis is given on Figure 3. Studies from multiple disciplines, including genetics, histopathology, cell biology and animal models, have provided what seems like an overwhelming support for the amyloid cascade hypothesis.

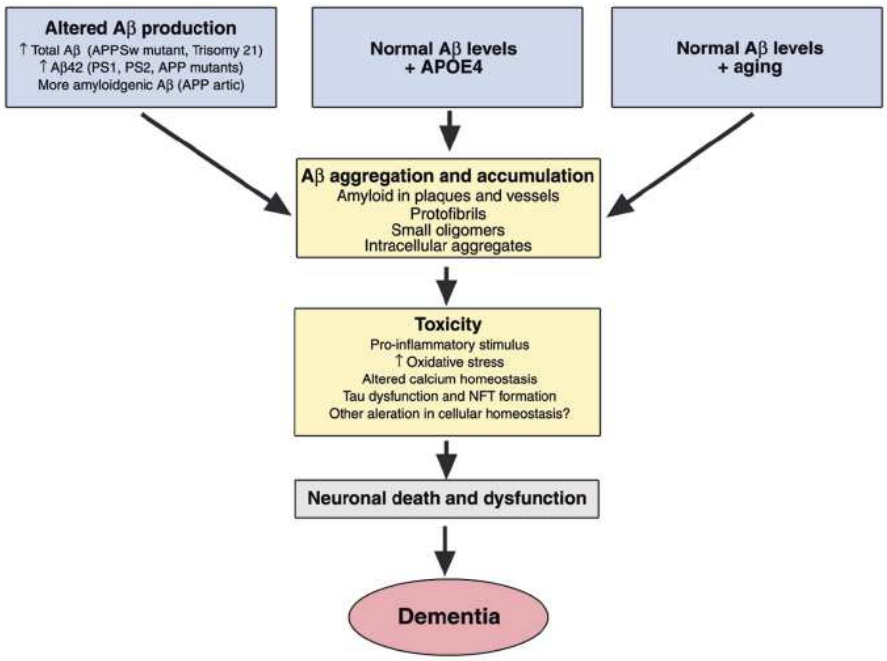


**Figure 3.** An overview of amyloid cascade hypothesis. Aβ aggregation as the cause of AD. Besides known genetic pathways (altered Aβ production leading to FAD and APOE4), a pathway in which normal Aβ levels in the context of normal aging may lead to Aβ accumulation is shown [24].

The strongest evidence for a pathogenic role for APP or Aβ comes from genetic studies of early-onset FAD. Several FAD mutations have been found in the APP gene. All of these mutations have been found to cluster close to the amyloid sequence in APP. All the FAD mutations in the APP gene result in increased production of $A\beta_{1\text{-}42/43}$ [25-27]. More than 70 FAD mutations in the presenilin 1 and presenilin 2 genes have also been reported [6]. Presenilin 1 and 2 are the catalytic core of the γ-secretase complex [28]. The common feature of all these mutations is that they also cause an increase in the production of $A\beta_{1\text{-}42/43}$ [29].

By definition Aβ plaques are the essential component of AD pathology. And indeed, one carefully controlled study with low sample size showed a strong correlation between cognitive dysfunction and Aβ plaque load in the entorhinal cortex [30]. However in general it has been shown that there is a poor correlation between the "plaque load" with the degree of dementia and elderly non-demented people also sometimes have a significant plaque load [31]. It has also been shown that in young patients with AD there is a strong correlation between dementia severity and plaque and tangle burden, whereas this association is not found in elderly patents with the disease [32]. In APPswe/PS1d9xYFP (B6C3-YFP) transgenic mice it was shown that plaques

formed quickly and within 1-2 days of the plaques appearance, microglia are activated and recruited to the site. Progressive neuritic changes ensue, leading to increasingly dysmorphic neuritis over the next days to weeks. That shows that plaques are critical mediators of neuritic pathology [33].

The amyloid cascade hypothesis states that the Aβ aggregation is the cause of AD but it does not explain in detail which aggregates are toxic and does not elucidate at all why aggregation occurs.

Tissue culture studies *in vitro* have demonstrated the neurotoxic nature of Aβ peptides. Both *in vitro* and *in vivo* Aβ assembles into different types of supramolecular structures ranging from small soluble oligomers to insoluble amyloid fibrils. A number of early studies showed that fibrillar Aβ is neurotoxic. But monomeric Aβ was incapable of producing such changes. These deleterious changes were also observed *in vivo* when fibrillar Aβ was injected into mouse brains [34]. However soluble oligomers have now been identified as the main source of neurotoxicity [18]. *In vivo* small stable oligomers of $A\beta_{42}$ have been isolated from the brains of AD patients. The large increase (up to 70-fold) in extractable soluble oligomers appears to be specific of brain regions responsible for cognitive functions that are impaired in AD patients, being present in the frontal cortex and not detectable in cerebellum [35]. The origin of the oligomers is not clear – *in vitro* they appear only in highly concentrated solutions at low temperatures [36]. However *in vivo* Aβ concentrations are lower and therefore fibrillisation is more likely to occur.

A recent study showed that natural lipids destabilize and rapidly resolubilize mature fibers and that the equilibrium is toward soluble amyloid protofibrils. They found that these protofibrils are toxic to primary neurons and cause memory impairment and tau phosphorylation in mouse. Therefore amyloid plaques may potentially serve as a major source of soluble toxic aggregates [37].

Despite the significant advances in AD research made in the last decade, the nature of the toxic form of Aβ involved in early AD pathology and also whether it is the fibrillar or the non-fibrillar peptides that are the most deleterious to neurons remain controversial issues[38].

## 1.3. Zinc and copper in brain.

Metals are distinguished by their ionization and bonding properties. They are widely distributed in nature and in biological systems. They can be broadly classified as either “biometals” or “”toxicological metals” based upon whether they have a functional role, or are detrimental to the organism. The metal ion content of the brain is stringently regulated with virtually no passive flux of metals from the circulation to the brain

Copper is necessary for the activity of a number of physiologically important enzymes. As a cofactor in multiple redox reactions, Cu is also involved in the production of potentially damaging radical species through Fenton or Haber-Weiss reactions. For this reason, all organisms have redundant mechanisms for controlling Cu concentrations [39]. Copper is distributed throughout most regions of the brain and is most abundant in the basal ganglia. Under normal physiological conditions copper ions are bound to Cu enzymes or proteins. In some neurons, copper is released at the synapse. The concentration of Cu in the synaptic cleft can be as high as 15 – 100 μM [40, 41]. But the nature of the released copper is not known. The synaptic copper release has been studied using tetrakis(4-sulfophenyl)porphine (TSPP). The concentration of Cu in the synaptic cleft after depolarization was found to be 3.2 μM. These results were confirmed using inductively-coupled-plasma mass-spectrometry (ICP-MS) and the copper concentration was found to be 14 μM. These results differ because ICP-MS also measures copper ions bound to proteins with lower $K_D$ values than TSPP ($K_D$ = 0.43 μM) [42].

Zinc is the most abundant trace element in the body after iron and considerably more abundant than copper. The bulk of body zinc is tightly bound within cellular metalloenzymes and Zn finger proteins. This fixed pool of Zn turns over very slowly and is mainly responsible for housekeeping functions in cellular metabolism and gene expression. The remaining 10 – 15% of Zn comprises of more dynamic pools that are readily depleted in Zn deficiency. While fixed Zn is distributed uniformly throughout the body, labile Zn is concentrated in certain tissues and in specific regions within tissues [43]. The brain has the highest zinc content compared with other organs. The average of total brain zinc is estimated to be approximately 150 μM. Free zinc ion concentration in the cytosol in cultured neurons is submicromolar and about 500 nM in

the brains extracellular fluids [43]. However up to 15 % of zinc in the brain is in the synaptic vesichles. The concentration of zinc upon synaptic transmission is between 200-300 μM [44, 45] Most of the zinc-ergic neurons are in the brain regions that are affected by AD [46, 47] .

## 1.4. Metal hypothesis of Alzheimer's disease

Other neurochemical events apart from Aβ production may also contribute to Aβ deposition and toxicity in AD. If elevated cortical Aβ concentrations are to be solely responsible for the deposition of Aβ, it would be difficult to explain why the depositions are focal (related to synapses and the cerebrovascular lamina media) and not uniform in their distribution, especially because APP and Aβ are ubiquitously expressed. Moreover Aβ deposition is an age-dependent phenomenon, Aβ production however does not appear to increase with age [48].

The Aβ aggregation and toxicity is thought to be connected with metals – this hypothesis does not contradict the previous one, instead it tries to explain why aggregation occurs and why the aggregates are toxic. There is considerable evidence for there being an imbalance in transition metal homeostasis in AD. Zinc, copper and iron are found in high concentrations (~1 mM) in the amyloid plaques [2]. Aβ directly coordinates copper and zinc, but not iron or other metal ions within the cores of plaques [49]. The toxicity of Aβ bound copper ions in the presence of natural reducing agents (ascorbic acid) is well documented. As Aβ associated copper is electrochemically active, it might also induce the production of reactive oxygen species causing oxidative stress in AD [50]. Aβ copper complexes are toxic to neuronal cells *in vivo* in the presence of a reducing agent [51].

A role for synaptic zinc in Aβ deposition and amyloid formation has been demonstrated in transgenic mice, which express human APP. They serve as a model for AD, because they are able to develop amyloid plaque pathology. If they lack the zinc-transporter ZnT3 that transports Zn into synaptic vesicles, then the plaque load is reduced by approximately 50%. Hence zinc contributes to the amyloid deposition [52].

In a rabbit model for AD, trace amounts of Cu(II) in the drinking water of cholesterol-fed rabbits induced the accumulation of Aβ formation of senile plaques and retardation of the rabbits ability to learn a difficult task [53]. When transgenic strains of *Caenorhabditis elegans*, that overexpress Aβ intracellulary in muscle cells and form Aβ aggregates, are grown in the presence of Cu(II) the number of aggregates increases [39]. However, an advantageous effect of Cu(II) on AD pathogenesis has also been clearly demonstrated. It has been shown that bio-available Cu(II) is beneficial to transgenic mice over-expressing human full-length APP carrying the Swedish/London mutation. Cu(II) treated mice had a detectable reduction of amyloid plaques and did not show the premature lethal phenotype [54].

Studies from different fields show that Cu(II) and Zn(II) are connected with aggregation but the effect and the mechanism is incompletely understood.

### 1.4.1. Affinity of Aβ peptides towards Cu(II) and Zn(II)

The metal binding ability of proteins and peptides is an important parameter in biology. It gives information about the physiological significance of the interaction of a protein/peptide with a given metal ion. A binding affinity that is too low may indicate that the peptide is not able to bind the metal ion *in vivo* due to the presence of other ligands with stronger affinities. The affinity of Cu(II) and Zn(II) ions for the Aβ peptides is also crucial in order to design chelators able to retrieve the metal ion from the Aβ peptides.

The Aβ peptide binds metal ions via the three histidine residues [49]. Some structures have been determined for the shorter versions of Aβ (Figure 1). Cu(II) forms a 1:1 complex with Aβ [55, 56]. At higher copper concentrations a second ion binding has also been seen [57]. For Zn(II) stoichiometry from 1:1 [58] to 3:1 [59] has been observed. The formation of oligomeric complexes with histidine residues originating from different molecules has also been suggested [60, 61].

The apparent $K_D$ values for Cu(II)-Aβ complex show a very large variation from 0.1 nM up to 10 μM. This is very likely due to the variety in techniques used for the determination and also to different experimental conditions (buffers used). In the first

stage of our study of the metal-Aβ interactions it was determined that the conditional (extrapolated to zero buffer concentration) $K_D$ value is 35 nM [62] This is close to the affinity of copper towards amino acids and other low-affinity ligands and proteins present in extra-cellular environment [63]. The concentration of synaptically released copper ions might be sufficient for the formation of Cu(II)-Aβ complex. This complex formation may significantly affect the homeostasis and metabolism of Aβ peptides and may lead to the insertion of Cu(II) ions to amyloid plaques [62].

The reported values of Zn(II)-Aβ complex are between 1 and 300 μM. Higher values originate from Tyr 10 fluorescence measurements, other methods give values in a ranges of 1 - 20 μM [64]. The interaction of Zn(II) with Aβ depends on the incubation time and mixing conditions. Comparing different methods it can be seen that the micromolar constants were detected in experiments with longer incubation compared with the fluorescence measurements. Therefore it is possible that micromolar Zn(II) binding affinities are characterising zinc-induced oligomers or aggregates of Aβ. We demonstrated that the Zn(II)-Aβ complex with affinity of 60 μM transformed into a high-affinity complex ($K_D$ ~ 2 μM) in 30 minutes. Considering the $K_D$ values it can be concluded that the formation of a Zn(II)-Aβ complex is probable in certain brain areas which contain synapses of zincergic neurons [62].

The affinity measurements confirmed that the interaction of Zn(II) and Cu(II) ions with Aβ peptides may occur in certain brain areas and therefore these metal ions might affect Aβ aggregation *in vivo*.

### 1.4.2. Metals and Aβ aggregation

The generally accepted model for growth of amyloid fibrils is the nucleation-elongation model, where the rate-limiting step is the formation of a nucleus (“seed”) through the self-association of monomers, followed by the rapid growth through addition of monomers to the nucleus leading to fibrils, and finally a steady state when the aggregate and monomers appear to be in equilibrium [65]. For $Aβ_{40}$ an equilibrium point of 0.7 - 1.0 μM has been obtained [66], for $Aβ_{42}$ however it is known to be smaller but it has not been determined experimentally.

There is a consensus that acquiring the extended β-conformation is pivotal for Aβ fibrillation and indeed, in the fibrils Aβ peptides are to a great extent in β-conformation and form interchain hydrogen bonds with neighboring peptide units by constituting a cross β amyloid core of the fibril [67, 68]. The organisation of the cross β unit in fibrils may vary with conditions [69] but the common feature is that residues 10-23 and 30-40 are forming beta structure as shown in Figure 1.

Influence of zinc and copper ions on aggregation of Aβ peptides has been intensively studied over the last decade; nevertheless, many important aspects like the effect of metal ions on aggregation kinetics and the effect of chelators on metal-induced aggregation of Aβ are still elusive.

In the early studies the metal ions have been reported to enhance the rate of Aβ fibrillation and metal chelators acted in an opposite direction by reversing the aggregation state of Aβ [70-72]. Later it was found that the metal-induced Aβ aggregates are dominantly non-fibrillar [73-75], however, enhanced formation of fibrillar structures in the presence of Zn(II), Cu(II) and other metal ions has also been observed [76, 77]. It has even been suggested that the presence of trace levels of biometals is absolutely necessary for the fibrillation of $A\beta_{40}$ to occur [78]. Reasons for the inconsistency in results are unknown. It is also unknown, which amino acid residues of Aβ peptides mediate the effect of Zn(II) and Cu(II) on the aggregation.

The putative causative role of metal ions in AD pathology provides the basis for a relatively new therapeutic approach for AD called “metal chelation therapy” [48, 79] that relies on the assumption that metal ions cause aggregation of Aβ peptides and predicts that removal of metal ions, especially Cu(II) and Zn(II), from amyloid plaques by metal chelators should lead to the solubilization of the plaques. This therapeutic approach has been tested in animal experiments by using weak metal chelators like clioquinole (CQ) and its derivatives, which indeed acted as potentially therapeutic drugs by reducing plaque load in transgenic mice models of AD [79, 80]. In cellular and animal experiments it has been demonstrated that besides metal chelating ability, CQ has other systematic effects at the cellular and organism level [81]. Moreover, a considerable criticism of the metal chelating therapeutic approach has arisen recently on the basis of *in vitro* studies of Aβ fibrillation [82]. Hence, it is evident that the evaluation of the metal chelating therapeutic approach should rely on the proper

understanding of two fundamental aspects – (i) the effect of metal ions on the aggregation of Aβ peptides; (ii) the effect of metal chelators on metal-induced Aβ aggregates, both of which are currently incompletely understood.

It is clear that fibrillation is not the only aspect of AD that is connected with metal ions, but studying this aspect might provide information about the prospect of the metal chelation therapy.

## 1.5. Methods for the detection of protein fibrils and monitoring fibrillation kinetics.

The formation of fibrils with characteristic cross-beta structure is not a unique property of Aβ, approximately 100 peptides and proteins can form amyloid fibrils with characteristic similar morphology and tinctoral properties. The morphology is studied by transmission electron microscopy (TEM) that is not applicable for kinetic measurements.

Quantitative analysis of the kinetics of fibril formation requires both – well characterized protein preparations and appropriate monitoring techniques, as significant variations in the degree of aggregation in the initial solution may lead to large experimental irreproducibility. Several techniques have been employed in the study of fibrillation of proteins, including quasielastic light scattering, turbidity, analytical ultacentifugation, size exclusion chromatography, TEM and atomic force microscopy [83-86].

One of the most widely used techniques for registration the fibril formation is Thioflavin T (ThT) fluorescence. The benzothiazole dyes molecule consists of a pair of benzothiazole and benzaminic rings freely rotating around a shared C-C bond (shown as φ on Figure 4). Should the free rotation of ThT be hindered, the molecule exhibits a strong fluorescence. This is particularly the case of ThT-amyloid complexes, wherein the rotation is effectively blocked and quantum yield of the fluorescence is at its highest [87]. In the presence of fibrils, ThT gives rise to an excitation maximum at 450 nm and enhanced emission at 482 nm, whereas unbound ThT is essentially non-fluorescent at

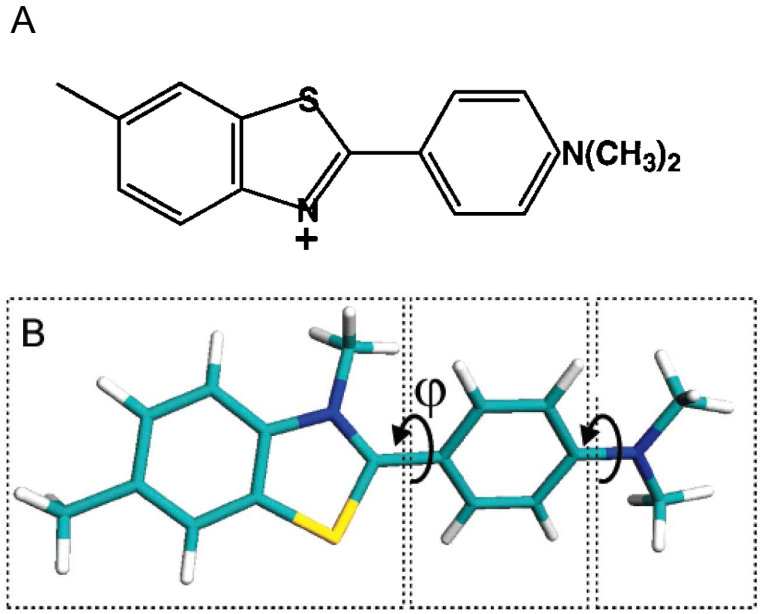


**Figure 4.** Chemical structure (A) and spatial model (B) of ThT cation. S, C and N atoms are shown in yellow, cyan and blue, respectively [88].

these wavelengths. ThT is believed to interact relatively specifically and rapidly with amyloid fibrils, and the binding is independent of the primary structure of the protein. Only the multimeric fibrillar forms, not multiple β-sheet domains in native proteins, fluoresce with ThT [89].

Different experimental setups are used in the practical application of the ThT method used in the literature [90, 91] Most of them use discontinuous setup where aliquots from the aggregation mixture are pipetted to ThT solution for measurements. However, for kinetics measurements this method is material and also time-consuming. Especially considering that the fibrillation of defibrillated peptide samples tends to take days if not weeks [91, 92]. There is evidence that small ThT concentrations do not interfere with fibril formation [93] and the fibrillation process can be speed up by agitation [94, 95].

## 1.6. Objectives of the present work

There is accumulating evidence that Zn(II) and/or Cu(II) participate in the amyloidogenesis *in vitro* and *in vivo*. Considering the impact of the metal ions on the

fibrillation of Aβ peptides a therapeutic strategy, metal chelation therapy, has been proposed. Despite of the great interest the effects of metal ions and chelators on the peptide aggregation/fibrillation are still obscure.

The main objective of this project was quantitative determination of the effects of zinc and copper ions as well as some representative metal chelators on the fibrillation of Aβ peptides. For this purpose a fast and reliable method for measuring Aβ aggregation has to be elaborated by improving currently used experimental ThT based methods. A series of experiments were planned to validate the relevance of clinically used metal chelators in the context of metal chelation theraphy of AD.

# 2. MATERIALS AND METHODS

## 2.1. Materials

The following reagents were used:
lyophilized $A\beta_{42}$ peptides NaOH salts or HFIP forms (ultra pure, recombinant) – rPeptide (Athens, USA)
HEPES, Ultrapure, MB Grade – USB Corporation (Cleveland, USA)
1,1,1,3,3,3-hexafluoro-2-propanol (HFIP), Zincon, Thioflavin T, α-cyano-4-hydroxycinnamic acid, trifluoroacetic acid, $CuCl_2x2H_2O$, EDTA, GSH, glutamate, glycine, cysteine, clioquinole and histidine hydrochloride – Sigma-Aldrich (St. Louis, USA)
$ZnCl_2$ and NaCl were extra pure – Scharlau (Barcelona, Spain).
Metallothionein-2 and -3 were in-house products expressed and purified according to the protocol described in [96].

## 2.2. Sample preparation

Stock solution of Aβ peptides was prepared as follows: 1 mg of the peptide was dissolved in HFIP at a concentration 500 μM to disassemble preformed aggregates [97]. The solution was divided into aliquots, HFIP was evaporated in vacuum and the tubes with the peptide film were kept at -80° C until used. Before using the Aβ HFIP film was dissolved in water containing 0.02 % $NH_3$ at a concentration of 10-20 μM. After 10 minutes of incubation the Aβ stock solution was dissolved with buffer and used for experiments. The quality of the peptide was checked with mass-spectroscopy on Ettan$^{TM}$ MALDI TOF MS machine.

Zincon powder was dissolved in Milli-Q water. The concentration of the obtained solution was found by measuring optical density at 620 nm ($\varepsilon$ = 23 500 $cm^{-1}$ $M^{-1}$) on Shimadzu UV-2401 PC spectrophotometer.

The stock solutions of metals, buffers and ligands were made using MilliQ water. The concentration of the zinc solution was checked with atom absorption spectroscopy on a Perkin Elmer 3100 instrument.

## 2.3. Fluorescence Spectroscopy

Fluorescence spectra were collected on a Perkin-Elmer LS-45 fluorescence spectrophotometer equipped with a magnetic stirrer. Fibrillation was monitored using ThT fluorescence.

$A\beta_{42}$ was diluted in 20 mM HEPES and 100 mM NaCl, pH 7.4 containing 3.3 μM of ThT to a final concentration of 5 μM. When needed an appropriate amount of Zn(II) or Cu(II) and different metal chelators was added in the form of freshly diluted solutions. 400 μl of each sample was incubated in a 0.5 cm path length quartz cell and agitated with a magnetic stirrer at 250 rpm. ThT fluorescence was measured at 480 nm using excitation at 440 nm.

The aggregation parameters were determined by fitting the plot of fluorescence intensity versus time to Boltzmann sigmoid curve

$$y = \frac{A_2 - A_1}{1 + e^{(x - x_0)/dx}} + A_2 , \qquad (1)$$

where $A_1$ is the initial fluorescence level, $A_2$ corresponds to the fluorescence at maximal fibrillation level, $x_0$ is the time when fluorescence is reached half maximum and dx is the time constant reciprocal to the rate constant of the fibril elongation *k*. This formula is not related to the underlying molecular events, but is a convenient method for the comparison of fibrillation kinetics.

$IC_{50}$ values were calculated according to hyperbolic curves:

$$k = k_0 - \frac{k_0 \times [Me^{2+}]}{[Me^{2+}] + IC_{50}} , \qquad (2)$$

where $[Me^{2+}]$ is the metal concentration, $k_0$ corresponds to the rate constant with no metal ions and *k* is the rate constant in the presence of metal ions.

For the detection of intrinsic tyrosine fluorescence of Aβ peptides, excitation at 270 nm was used and the emission spectra were recorded in the range of 290-360 nm. For calculations emission values at 305 nm were used. Before calculating all curves were smoothed with moving average method (step 5).

The titration of Aβ with copper ions was carried out in a 0.5 cm path length quartz cell without continuous stirring by adding 1-2 μl aliquots of stock solutions of the metal salt to the 400 μl of the peptide solution. After each metal addition the solution was stirred 10 s and the average fluorescence intensity was measured over a 10 s period. In the control experiments the intrinsic fluorescence of the peptide was constant for at least 30 minutes. Thus, the peptide solution is stabile and the changes in the fluorescence upon addition of metal salts are caused by the binding of metal ions to Aβ. At the end of the metal titration experiments the reversibility of the fluorescence changes was checked by adding 50 μM histidine as a metal chelator to the reaction mixture. To check the presence of aggregates at the end of metal-titration experiments the solution was centrifuged at 10,000 g for 15 minutes, 50 μM histidine was added to the supernatant and Aβ fluorescence was measured and compared to that of the initial sample.

The dissociation constants of the Cu(II)-Aβ complexes were calculated by fitting the titration data to the following equation:

$$I = I_0 + \frac{0{,}5 \times (I_0 - I_\infty)}{[A]} \times \left( [A] + [Cu^{2+}] + K_D + \sqrt{([A] + [Cu^{2+}] + K_D)^2 - 4 \times [A] \times [Cu^{2+}]} \right) \quad (3)$$

where [A] and [$Cu^{2+}$] are the total concentrations of the peptide and Cu(II) ions, $K_D$ is the dissociation constant of Cu(II)-Aβ complex and $I_0$, I and $I_\infty$ are the fluorescence intensities of the peptide sample in the absence, the presence, and the saturation of Cu(II) ions.

## 2.4. Transmission Electron Microscopy (TEM)

The grids were placed on an adhesive solid surface and 3 μl of previously centrifuged (30 min, 12000 g) peptide solution was pipetted on each grid and let air-dry. Then drops of 2% uranylacetate were spotted on a parafilm plate and grids were placed on them

with the upper side down (to bring the probe and the contrasting solution in contact). Probes were kept in uranylacetate for 10 min, then removed and washed with milliQ water. After that, excess water was removed with a filter paper and the grids were placed into a special carrier. TEM images from the samples were created on SELMI-SUMY EM-125 instrument at 75 kV accelerating voltage and recorded onto high resolution, 6x9 mm negative film.

## 2.5. Metal binding studies using Zincon

$A\beta_{42}$ was diluted in 20 mM HEPES and 100 mM NaCl, pH 7.4 to a final concentration of 4 μM with different concentrations of Zn(II) and Cu(II). The samples were incubated at room temperature and centrifuged at 10,000 g for 5 min. The concentration of free metal ions was determined by using a colorimetric dye Zincon. Zincons chemical structure is shown on Figure 5. Zincon forms a 1:1 complex with the metal ion, which absorbs at 620 nm (ε=23 500 $cm^{-1}$ $M^{-1}$ at pH 7.4). 50 μl of the supernatant was added to the Zincon solution and the OD was measured at 620 nm with GENios Pro reader (Tecan, Switzerland).

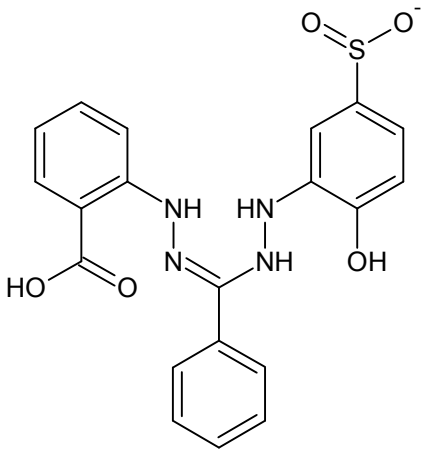


**Figure 5.** Chemical structure of Zincon.

# 3. RESULTS

## 3.1. Elaborating of the ThT method for monitoring the Aβ fibrillation

First the experimental conditions for fast and reproducible monitoring of $A\beta_{42}$ fibrillation were established.

Aβ peptide can be a very challenging reagent with which to work. Significant lot-to-lot variability affects aggregation behaviour. The increase in ThT fluorescence for different preparations of Aβ is shown on Figure 6. Lyophilized Aβ preparations without HFIP pre-treatment showed comparably high initial ThT-fluorescence levels indicating high content of fibrillar material. The initial fluorescence varied for different lots of the peptide. On the other hand, HFIP form of the peptide showed typical aggregation curve with initial lag time lasting up to 10 minutes when used immediately after solubilization in aqueous ammonia. After incubation of the alkaline peptide solution for approximately two hours the initial lag-period disappeared, however, even in the next day the initial ThT fluorescence of the preparation was low.

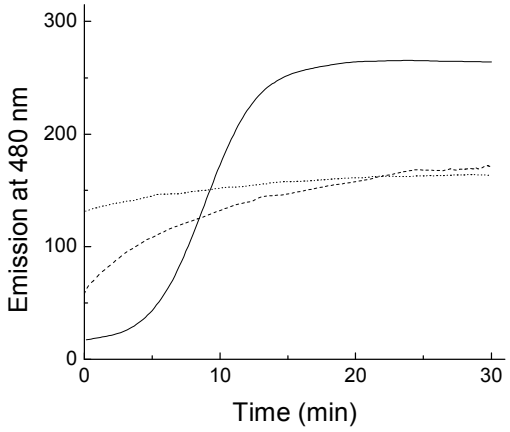


**Figure 6.** The effect of Aβ preparation on the fibrillation of $A\beta_{42}$. The aggregation of 5 μM $A\beta_4$ HFIP (—), NaOH Lot #: 9260542N (···) and NaOH Lot #: 5030742N (- -) form in 20 mM HEPES, 100 mM NaCl, pH 7.4, at 25°C with continuous agitation in the presence of 3.3 μM ThT.

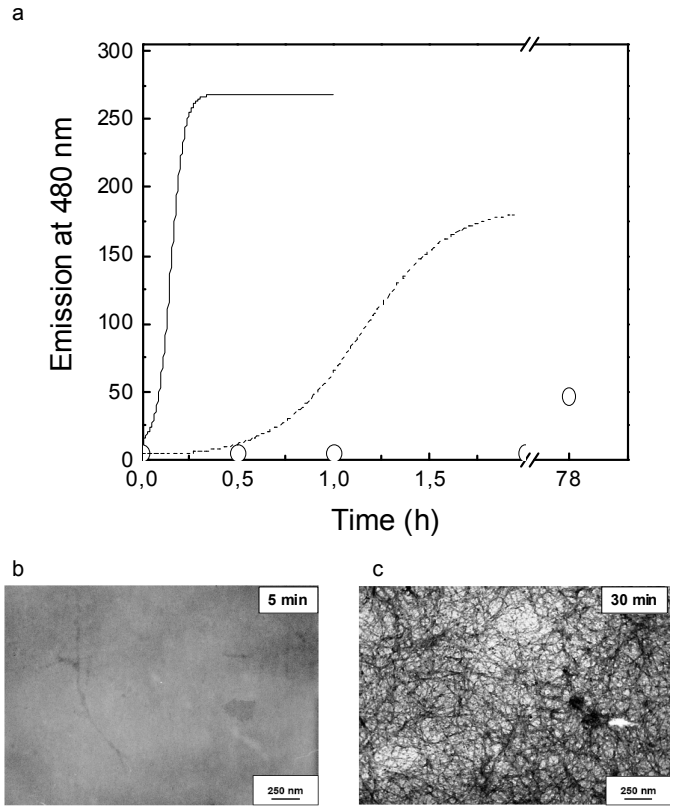


**Figure 7.** The effect of agitation on the fibrillation of $A\beta_{42}$. The aggregation of 5 μM $A\beta_4$ (a) with continuous mixing (—), impulse mixing (···) or without mixing (○) in 20 mM HEPES, 100 mM NaCl, pH 7.4, at 25°C in the presence of 3.3 μM ThT. TEM images from the sample with continuous mixing taken after 5 min (b) and 30 min (c) of incubation.

After pre-treatment of lyophilized peptides with HFIP the peptide preparation shows similar behaviour to the commercial HFIP form. The HFIP forms of Aβ showing negligible initial ThT fluorescence e. g. monomeric Aβ peptides were used in further experiments. The fresh HFIP-treated peptide did not show presence of oligomers in SEC analysis and did not contain fibrillar material when tested by TEM.

It was found that with defibrillized Aβ the agitation of the incubation mixture is critical for obtaining fast and reproducible fibrillation at low micromolar Aβ concentrations. A fast increase in the ThT fluorescence according to a typical two-phase growth curve (Figure 7) was observed only with continuous agitation. In general the fibrillation of amyloidogenic peptides and proteins *in vitro* is a self-propagating process characterized by a sigmoidal growth curve where the initial lag phase is followed by the fast fibril growth due to the addition of monomers to the end of existing fibrils. Decreasing the mixing intensity by using periodical mixing or replacement of the stirrer rod by a

smaller ball decreased the rate of fibril growth significantly. When $A\beta_{42}$ was incubated without agitation the fibrillation process was extremely slow and only a slight increase in the ThT fluorescence of $A\beta_{42}$ solutions was observed during prolonged incubation (3-5 days). Fibrillation rate was in positive correlation with the stirring intensity and remained constant at stirring rates above 200 rpm. The kinetic curves of fibrillation were fitted to several sigmoidal functions including Avrami, Gompertz and Boltzmann equations and it was found that the latter (Equation 1) provides the best fit of the experimental data and allows calculation of rate constants for the fibrillation process. The occurrence of fibrillation was checked with TEM (Figure 7 b,c). It was shown that after five minutes of incubation when the ThT curve has a lag phase there are no fibrils present. But after 30 minutes fibrils are seen. It is interesting to note that continuous agitation was needed only in the initial "seeding" phase of fibrillation. Peptide preparations with high initial ThT reactivity that were not monomerized by HFIP and contained fibrillar seeds fibrillated also without seeding. Moreover, when the mixing was stopped after formation of sufficient amount of ThT-reactive fibrils from the HFIP-treated peptide, the fibrillation proceeded also under quiescent conditions. Thus, the agitation was needed for seeding process not for fibril elongation.

A shown on Figure 8 ThT concentration of 3.3 was found to be sufficient to detect fibrils. In order to carry out fibrillation with continuous monitoring in the presence of the fluorescent dye it is important that ThT in the concentrations used does not affect

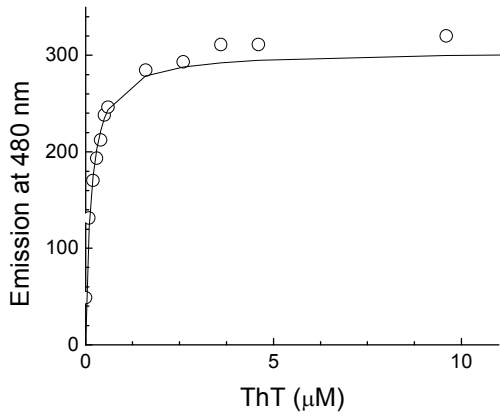


**Figure 8.** The titration of Aβ fibrils with ThT. Before titration 5 μM $A\beta_{42}$ was preincubated in 20 mM HEPES, 100 mM NaCl, pH 7.4, at 25°C with continuous agitation for 30 minutes.

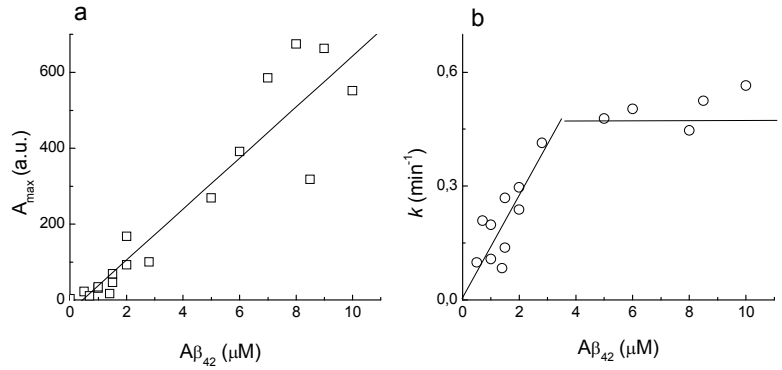


**Figure 9.** The effect of Aβ concentration on the fibrillation of Aβ$_{42}$. Aβ was aggregated in 20 mM HEPES, 100 mM NaCl, pH 7.4 at 25°C with continuous agitation in the presence of 3.3 μM ThT. ThT emission maximums at 480 nm (a), and $k$ values (b) with Boltzmann equation (Equation 1).

the process studied. It was established that an increase in the ThT concentration from 3.3 μM to 15 μM has no effect on the fluorescence intensity and on the rate of the fibril formation. And when ThT was added after 15 minutes of mixing the peptide in the cuvette then the final part of the reaction curve was also similar to that of the curve monitored in the presence of ThT from the beginning.

The concentration of the peptide solution is probably one of the most important factors affecting oligomerization processes. Figure 9 clearly indicates that level of the final ThT fluorescence is a linear function of peptide concentration, thus at the concentrations used the ThT fluorescence can be accounted as a measure of the amount of fibrils. The fibrillation rate constant $k$ = 0.52 ± 0.20 min$^{-1}$ was independent of the Aβ peptide concentration in the range of 2 to 10 μM. Parallel measurements at 5 μM Aβ revealed that the maximal ThT fluorescence is 276 ± 31 and the $k$ value 0.46 ± 0.09 (n = 9).

The effect of pH on the rate of fibrillation and maximal level of ThT fluorescence is presented in Figure 10. Both parameters did not changed significantly in the range of physiologically relevant pH. However, at lower pH the fibrillation rate decreased significantly.

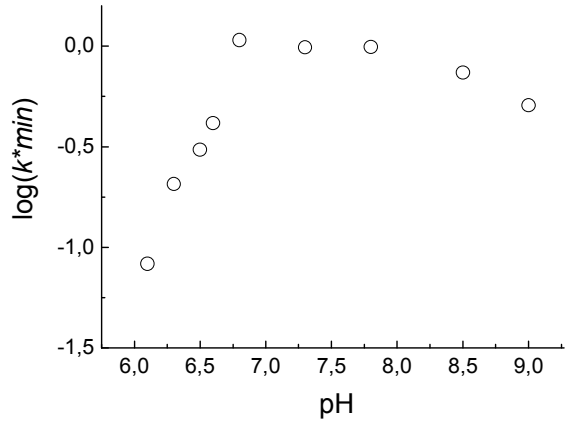


**Figure 10.** The effect of pH on the fibrillation of $A\beta_{42}$. The aggregation of 5 μM $A\beta_{42}$ in 20 mM HEPES, 100 mM NaCl, at 40°C with continuous agitation in the presence of 3.3 μM ThT, with various pH values.

Figure 11 shows the fibrillation curves at various temperatures. The effect of temperature on aggregation is similar to the data in the literature. It has been shown that at 4 $^{o}$C oligomerization occurs not fibrillation. At higher temperatures Aβ fibrils appear [36].

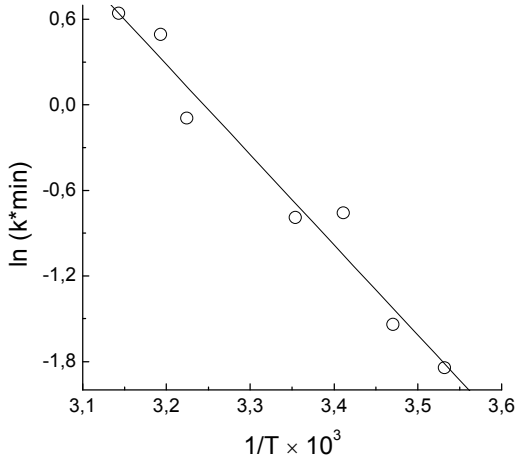


**Figure 11.** The effect of temperature on the fibrillation of $A\beta_{42}$. The aggregation of 5 μM $A\beta_4$ in 20 mM HEPES, 100 mM NaCl, pH 7.4, at 25°C with continuous agitation in the presence of 3.3 μM ThT at various temperatures. Line corresponds to Arrhenius plot

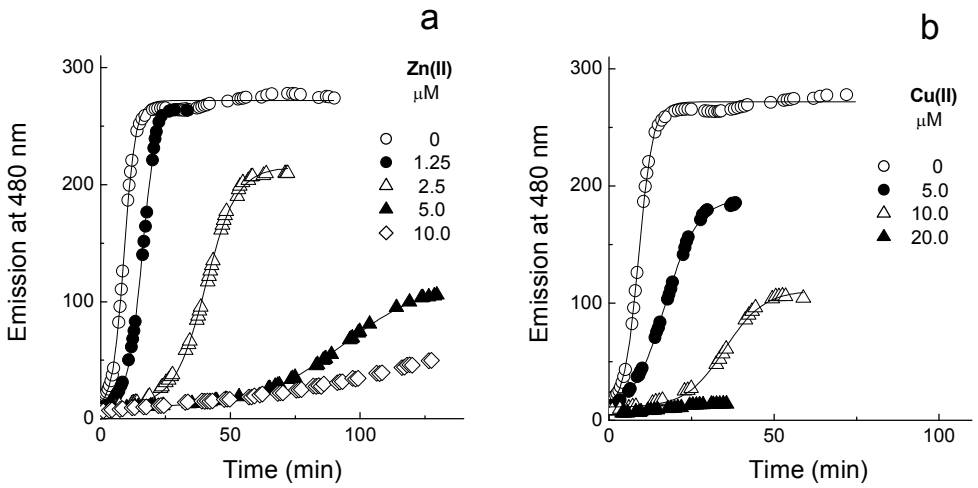


**Figure 12.** Effect of metal ions on fibrillation of $A\beta_{42}$ as followed by ThT fluorescence. (a) in the presence of Zn(II) and (b) Cu(II). Conditions: 5 μM of $A\beta_{42}$ in 20 mM HEPES, 100 mM NaCl at pH 7.3 was incubated at 25°C with continuous agitation in the presence of 3.3 μM ThT. Solid lines correspond to fits of the data to Boltzmann equation (Equation 1).

## 3.2. Effects of Zn(II) and Cu(II) on the formation of $A\beta_{42}$ fibrils

Both Zn(II) and Cu(II) exposed a pronounced inhibitory effect on $A\beta_{42}$ fibrillation curves shown in Figure 12. Metal ions decrease the fibrillation rate constant and increased the lag period of the process in a concentration dependent manner whilst at high Zn(II) and Cu(II) levels the final level of ThT fluorescence was also reduced. In the case of Zn(II) a twofold decrease of the fibrillation rate constant (considered as $IC_{50}$), was observed already in the presence of substoichiometric 1.8 μM concentration of Zn(II), whereas addition of two equivalents of Zn(II) almost completely suppressed the formation of ThT-reactive fibrils. The inhibitory effect of Cu(II) was characterized by $IC_{50}$ = 4.9 μM showing that Cu(II) is approximately three times weaker suppressor of $A\beta_{42}$ fibrillation than Zn(II). Our observation that Zn(II) and Cu(II) suppress the formation of fibrillar ThT-reactive aggregates is in qualitative agreement with the results by Yoshiike and colleagues, conducted under nonagitated conditions [73].

It was demonstrated further, that in parallel with suppression of $A\beta_{42}$ fibrillation metal ions initiated fast assembly of $A\beta_{42}$ into insoluble aggregates that sediment during

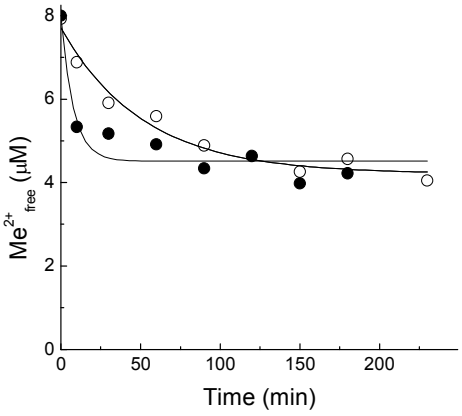


**Figure 13.** Coprecipitation of zinc (●) and copper (○) ions with Aβ $_{42}$. Fraction of metal ion disappearance from a solution of 4 μmol/l of Aβ in 20 mM HEPES, 100 mM NaCl at pH 7.3 and 25°C under quiescent conditions (the solution was mixed only by pipette before the aliquot was taken for metal determination).

centrifugation at 10,000g. Zn(II)-mediated assembly of the peptide was near-instantaneous whereas the precipitate formation with Cu(II) occurred within 30 min (Figure 13). It is essential to note that in the presence of metal ions continuous agitation was not necessary to ensure the fast peptide aggregation. This was also confirmed by fast increase in the light scattering of the peptide solution in the presence of these ions. The aggregation of HFIP-treated monomeric $A\beta_{42}$ into precipitable aggregates in the presence of metal ions was fast and as 4.2±0.2 μM of copper or 4.3±0.3 μM of zinc coprecipitated with 4μM of $A\beta_{42}$ it can be concluded that metal to peptide ratio in the metal-induced $A\beta_{42}$ aggregates formed in the presence of an excess of metal ions was approximately 1:1. However, after incubation of 5μM $A\beta_{42}$ for 10 minutes with 1 μM Zn(II) more than 60% of the peptide was found in the sediment after centrifugation, which indicates that Zn(II) can precipitate out superstoichiometric amounts of $A\beta_{42}$, when the peptide is at excess.

## 3.3. Effect of metal chelators on the inhibition of Aβ fibrillation by Zn(II) and Cu(II)

To get information about the reversibility of the metal effects and the strength of metal-amyloid interaction, we tested the effect of Zn(II) and Cu(II) ions on fibrillation of $A\beta_{42}$ in the presence of different metal-chelating agents. In the presence of 40 μM glycine 5

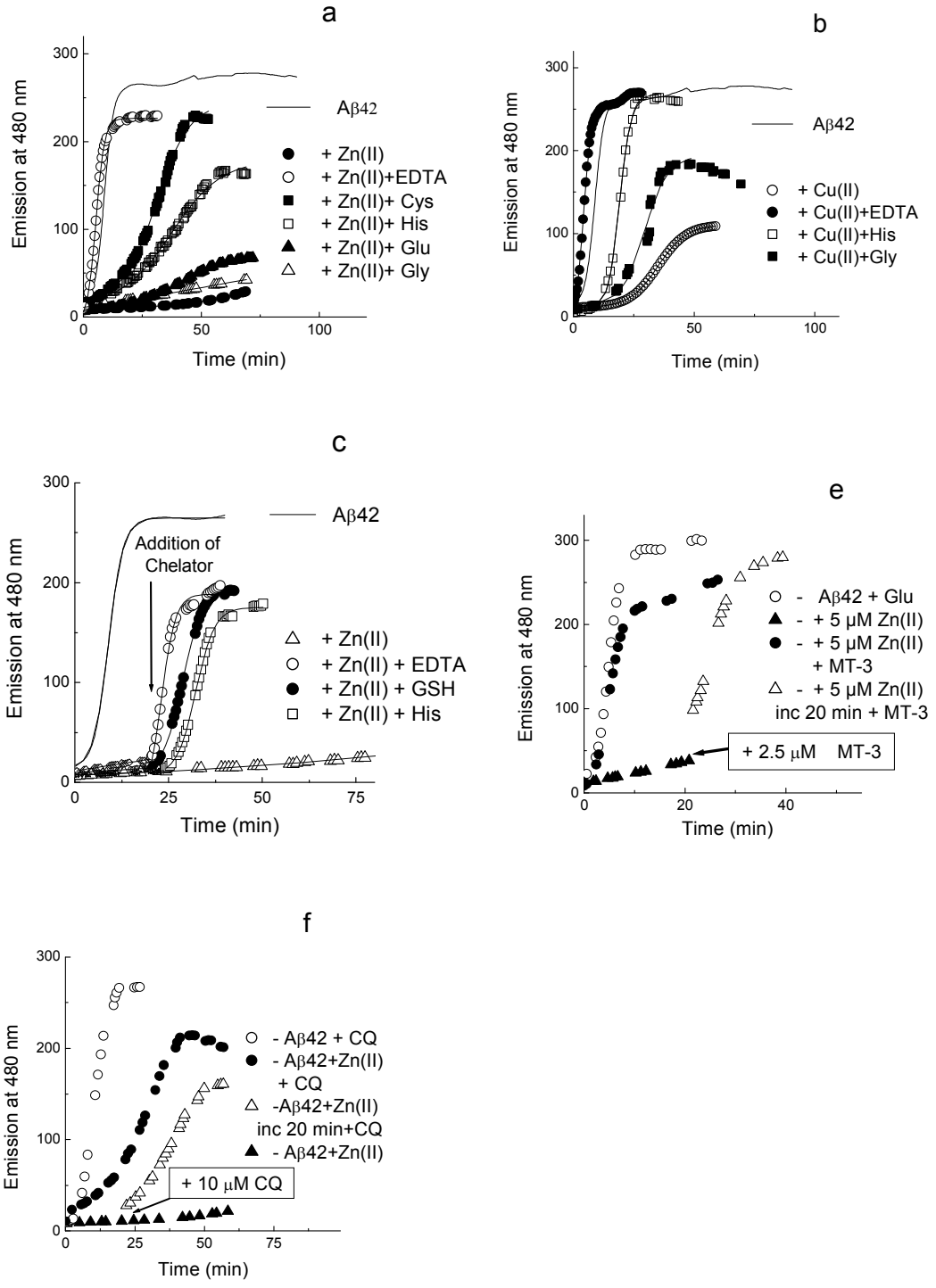


**Figure 14**. Effect of metal chelating agents on fibrillation of $A\beta_{42}$ in the presence of Zn(II) and Cu(II) ions. The chelators were added in the beginning of the fibrillation reaction (a,b) or after 20 min incubation of $A\beta_{42}$ in the presence of 10 μM Zn(II) (c); (d) Effect of apo-MT-3 on the fibrillation of $A\beta_{42}$ in the presence of 10 μM glutamate and 10 μM glutamate and 5 μM Zn(II). In the second experiment 2.5 μM MT-3 was added in the point indicated by an arrow. (e) Effect of CQ on the fibrillation of $A\beta_{42}$ alone and in the presence of 5 μM Zn(II). Time of CQ addition is indicated by an arrow. All reactions were carried out with 5 μM of $A\beta_{42}$ in 20 mM HEPES, 100 mM NaCl, 3.3 μM ThT at pH 7.3, 25°C.. Solid lines correspond to fits of the data to Boltzmann equation (Equation 1).

μM Zn(II) still inhibited fibrillation of $A\beta_{42}$ (Figure 14 a) However, only partial fibrillation was observed in the presence of 40 μM glutamate or histidine showing that these metal chelators compete with the peptide for Zn(II) ions. Cysteine also initiated the fibrillation in the presence of Zn(II), but the process was delayed. Addition of high affinity chelators like EDTA ($K_D^{ZnL}$ = 3.2 aM) and apo-metallothioneins (MT-2 and MT-3), ($K_D^{Zn}$= 0.14 pM) [98] completely abolished the inhibitory effect of Zn(II) on the $A\beta_{42}$ fibrillation. Chelating effect of amino acids correlates well with the metal binding affinity of the amino acids, which are characterized by β (logarithm of the stability constant of the corresponding $MeL_2$ complex) values for Zn(II) binding 9.2 (Gly), 9.5 (Glu) 11.8 (His) and 18.2 (Cys) [99]. The metal chelators prevented also Cu(II)-induced inhibition of $A\beta_{42}$ fibrillation (Figure 14 b) whereas their effect was more pronounced as in case of Zn (II): even Gly was able to reverse the inhibitory effect of 10 μM Cu(II) on fibrillation of $A\beta_{42}$.

Obtained results indicate that metal chelators prevent the formation of metal-induced $A\beta_{42}$ aggregates, however, it is also important to establish the effect of metal chelators on already formed metal-induced $A\beta_{42}$ aggregates. Addition of the high-affinity metal chelators to the fresh Zn(II)-induced $A\beta_{42}$ aggregates gave rise to a fast increase in the ThT fluorescence, reflecting a conversion of metal-induced aggregates to amyloid fibrils (Figure 14 c). Zn(II)-induced aggregates were converted to fibrils also in the presence of higher millimolar concentrations of His. Matured metal-induced aggregates (2-3 days old) were resistant to metal chelators and did not show any increase in the ThT fluorescence.

Aggregation of $A\beta_{42}$ was also carried out in an environment, mimicking the putative *in vivo* conditions for the peptide fibrillation in the regions of zinc-enriched glutamate-ergic synapses, composed from saline buffer, pH 7.4, containing Zn(II) and glutamate that are co-released into the synaptic cleft. Figure 14 d shows that 5 μM Zn(II) inhibits the fibrillation of 5 μM $A\beta_{42}$ in the presence of 10 μM glutamate. On the other hand, the presence of 1 μM apo MT-3 Zn(II) had no effect on the peptide fibrillation. Moreover, addition of brain specific apo-MT-3 to the Zn(II)-induced $A\beta_{42}$ aggregates induced rapid formation of ThT-reactive $A\beta_{42}$ fibrils (Figure 14 d).

To evaluate the metal-chelation potential of CQ - a putative drug candidate for metal chelation therapy of AD, we determined its effect on the $A\beta_{42}$ fibrillation as well as on the Zn(II)-induced aggregation of $A\beta_{42}$. Results presented in Figure 14 e show that CQ alone had no effect on the $A\beta_{42}$ fibrillation at concentrations up to 50 μM. In the presence of 10 μM CQ, 5 μM Zn(II) still inhibited fibrillation of the $A\beta_{42}$, however, inhibition was weaker as in the absence of CQ, indicating that CQ can not totally prevent Zn(II)-induced aggregation of $A\beta_{42}$. Addition of 10 μM CQ to the Zn(II)-induced $A\beta_{42}$ aggregates induced a relatively slow and limited fibrillation of the peptide (Figure 14 e) indicative of its limited ability to extract metal ions form Zn(II)-induced $A\beta_{42}$ aggregates and showing that CQ acts similarly to medium affinity metal chelators.

These results with metal chelators show that the inhibitory effect of Zn(II) and Cu(II) on fibrillation of $A\beta_{42}$ is reversible, whereas removal of metal ions from metal-induced $A\beta_{42}$ aggregates initiates peptide fibrillation. Only medium and high-affinity metal chelators were able to reverse the effects of metal ion on the $A\beta_{42}$ fibrillation, showing that the effect of metal chelators is non-specific and depends mainly on their metal binding affinity.

## 3.4 Fibrillation of His to Ala mutants of $A\beta_{42}$ in the absence and presence of Zn(II) and Cu(II).

In order to determine the role of His residues in the metal-induced aggregation of $A\beta_{42}$, we studied the fibrillation of all three His-Ala mutants of the $A\beta_{42}$ and compared the obtained results with the wild-type peptide (Figure 15 and Table 1). In the absence of metal ions the fibrillation kinetics of H13A and H14A peptides was similar to that for wt $A\beta_{42}$, whereas, in the case of H6A mutant the fibrillation was two times faster. The fibrillation rates of all mutant peptides in the presence of similar amounts of metal ions were similar. The $IC_{50}$(Zn) and $IC_{50}$(Cu) values were higher for the H13A

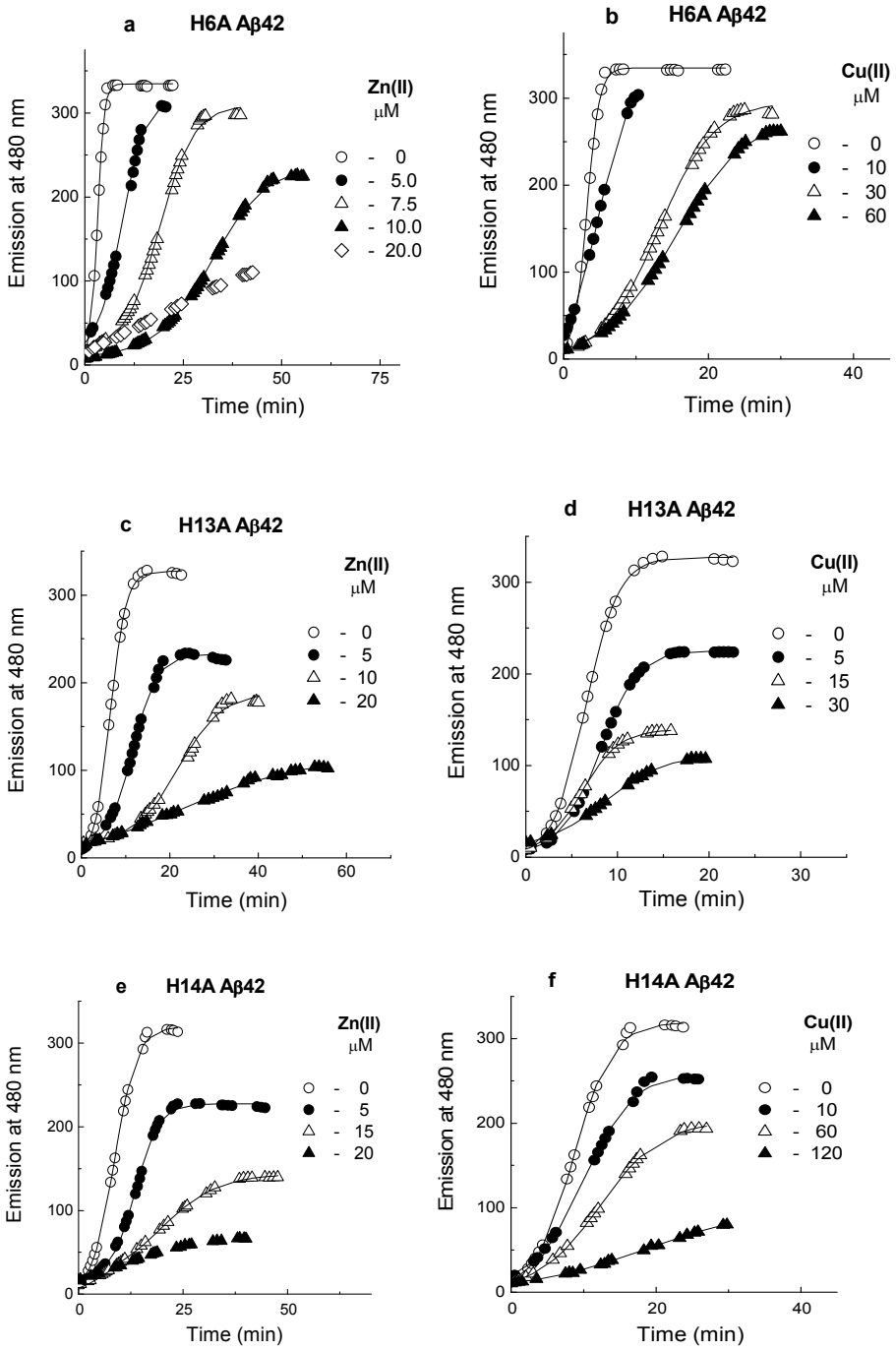


**Figure 15.** Fibrillation of His to Ala mutants of $A\beta_{42}$ in the presence of metal ions. (a) H6A $A\beta_{42}$ in the presence of Zn(II); (b) H13A $A\beta_{42}$ in the presence of Cu(II) (c) and H13A $A\beta_{42}$ in the presence of Zn(II); (d) H13A $A\beta_{42}$ in the presence of Cu(II); (e) H14A $A\beta_{42}$ in the presence of Zn(II); (f) H14A $A\beta_{42}$ in the presence of Cu(II). Conditions: 5 μM of mutant $A\beta_{42}$ peptides in 20 mM HEPES, 100 mM NaCl at pH 7.3 was incubated at 25°C with continuous agitation in the presence of 3.3 μM ThT. Solid lines correspond to fits of the data to Boltzmann equation (Equation 1).

and H14A mutant peptides in comparison with the $IC_{50}$ values for wild-type $A\beta_{42}$ (Table 1). In the case of the H6A mutant, the $IC_{50}$ values for Zn(II) and Cu(II) were

similar to those for wild-type peptide due to higher fibrillation rate in the absence of metal ions. The inhibitory effect of metal ions on the fibrillation of mutant peptides was also reversed by the addition of high-affinity metal-chelating agents like EDTA, which induced fast formation of ThT-reactive fibrils as observed for wild type peptide.

**Table 1.** Fibrillation of Aβ peptides in the absence and presence of metal ions

| $A\beta_{42}$ peptide | $k_0$ * $min^{-1}$ | Zn(II) $IC_{50}$, μmol/L | Cu(II) $IC_{50}$, μmol/L |
|---|---|---|---|
| wt | 0.45±0.09 | 1.8±0.9 | 4.9±1.1 |
| H13A | 0.60±0.01 | 5.2±1.4 | 43±16 |
| H14A | 0.37±0.01 | 11±6 | 78±25 |
| H6A | 1.16±0.05 | 1.75±0.1 | 7.5±1.6 |

IC50 values are calculated with Equation 2.

## 3.5 Affinity of His to Ala mutants of Aβ to metal ions.

The affinity of $A\beta_{42}$ mutants towards metal ions was determined by monitoring the intrinsic fluorescence of Y10, which is in case of wild-type peptides quenched by addition of Cu(II) and Zn(II) ions [62, 100, 101]. Addition of Cu(II) ions decreased also the intrinsic fluorescence of the mutant peptides, this is shown on Figure 16. The data was fitted to a quadric equation (Equation 3), this resulted in apparent dissociation constant ($K_D^{app}$) values for Cu(II)-peptide complexes equal to $K_D^{app}$ (H6A) = 2.55±0.60 μM, $K_D^{app}$ (H13A) = 0.88±0.20μM, and $K_D^{app}$ (H14A) = 3.59±0.60 μM. The $K_D^{app}$ values for H14A and H6A mutant peptides are considerably higher than $K_D^{app}$ = 0.76 μM for wild-type $A\beta_{42}$ under similar conditions [62] confirming their involvement in the formation of metal-peptide complex, however, the contribution of H13 to the Cu(II) binding affinity of $A\beta_{42}$ is surprisingly low as $K_D^{app}$ value for H13A mutant is similar to

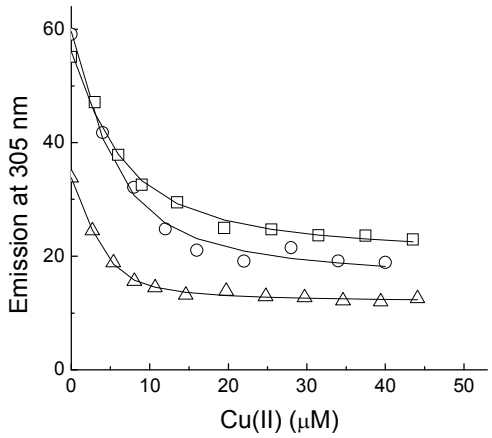


**Figure 16.** Intensity of the intrinsic fluorescence of $A\beta_{42}$ mutants as a function of added Cu(II). Titration of 4 μM $A\beta_{42}$ H6A (○), H14A (□) and H13A (△) was carried out at pH 7.3 and 25°C in 20 mM HEPES, 100 mM NaCl; Excitation at 270 nm.

that for wt $A\beta_{42}$. Intrinsic fluorescence of the His-Ala mutant peptides did not show any changes when Zn(II) ions were added to the peptide in the concentrations up to 0.5 mM. This does not necessarily mean that the metal-binding affinity of the mutant peptides is lower than 0.5 mM, since binding of Zn(II) ion may not affect the intrinsic fluorescence of the tyrosine residue in mutant peptides.

## 3.6 Characterization of Aβ complexes with transmission electron microscopy.

To confirm results obtained by ThT fluorescence the samples of $A\beta_{42}$ fibrils and metal-induced $A\beta_{42}$ aggregates were studied by TEM. No fibrils were detected in the samples of $A\beta_{42}$ before the appearance of ThT fluorescence (agitation for 5 min), whereas $A\beta_{42}$ samples showing high ThT fluorescence (agitation for 30 min) showed high content of fibrils (Figure 17) confirming that the increase of ThT fluorescence reflects peptide fibrillation in our assay. In $A\beta_{42}$ samples with added Cu(II) and Zn(II) ions, only a small amount of nonfibrillar aggregates was detected after short (~30 min) incubation. After prolonged incubation (~ 1 week) $A\beta_{42}$ samples with added Cu(II) and Zn(II) ions also exhibited fibrillar aggregates in TEM (Figure 17), confirming that the metal-induced $A\beta_{42}$ aggregates are converted slowly to $A\beta_{42}$ fibrils.

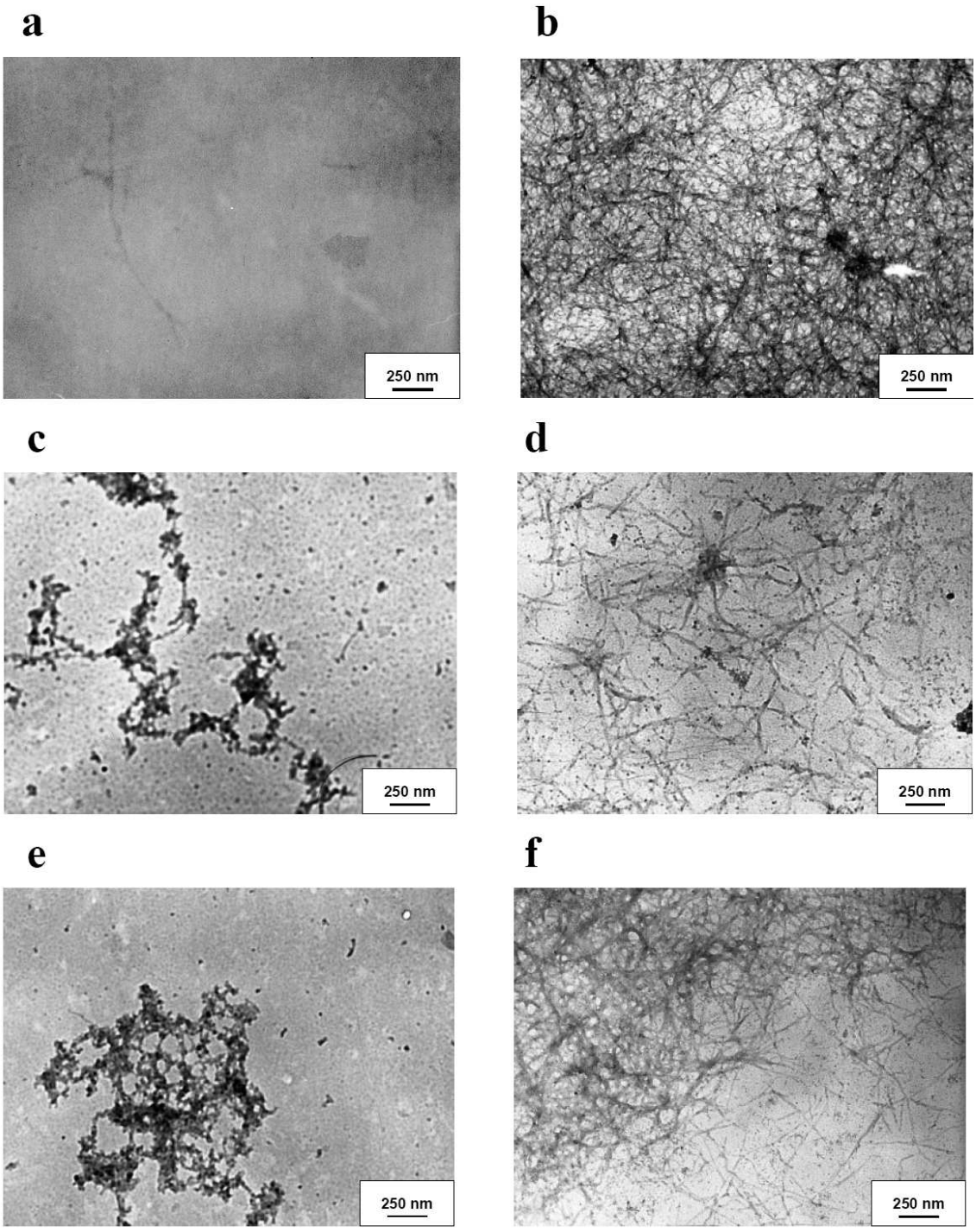


**Figure 17**. TEM images of $A\beta_{42}$ samples. (a) $A\beta_{42}$ agitated for 5 min ; (b) - $A\beta_{42}$ agitated for 30 min; (c) - $A\beta_{42}$ agitated with 5 μM Zn(II) for 30 min (d) same samples as in (c) incubated for 1 week. (e) $A\beta_{42}$ agitated with 5 μM Cu(II) for 30 min; (f) same samples as in (e) incubated for 1 week. Incubation conditions: 20 mM HEPES and 100 mM NaCl, at pH 7.3, 25°C.

# 4. DISCUSSION

The Aβ aggregation and fibrillation are crucial aspects in the development of AD. Studies of the fibrillation kinetics *in vitro* in the presence of various factors including metal ions can provide valuable information about the process and also provide clues for understand the role of endogenous metal ions and metal chelating agents in amyloid plaque formation in the brain.

***Aβ fibrillation in vitro***.

The rate of fibril elongation was consistent with first-order kinetics as confirmed by good fit of the experimental data to the latter half of the sigmoid. An interesting feature is the independence of corresponding rate constant on the peptide concentration above 2 μM. Similar phenomenon is earlier observed in the process of insulin fibrillation where under vigorous shaking the fibrillation curves were similar at different insulin concentrations but no explanation was provided for this phenomena by the authors [95]. The rate-constant characterizing the disappearance of monomers during fibrillar growth is suggested to be independent of the peptide concentration when the equilibrium between the peptide fibrillation-competent and incompetent conformations in the solutions is shifted towards the latter [102]. Most likely this suggests that the rate of fibril elongation is limited by obtaining an addition-competent structure in solutions (or any other monomolecular process) when the fibrillar seeds are present in sufficiently high concentration

A number of studies on unseeded amyloid fibril formation demonstrate a dramatic rate enhancement by stirring. This has been explained in many ways. Historically, it was suggested that agitation can fragment fibrils, which increases the number of ends available for nucleation [103]. However with Sup35 fragmentation could not be detected and it was suggested that agitation accelerates polymerization by dissociating overly large complexes and/or increases the collision of eligible complexes with each other and with fiber ends [104]. Also it has been suggested that the encounter frequency *in vitro* depends on the rate of stirring in a dramatic fashion when the nuclei become sparingly soluble or insoluble [103]. Our results showed that agitation is important only in the initial phase of the reaction which is in agreement with the explanation that agitation fragments fibrils.

The reproducibility of the duration of the lag phase was not good enough to carry out a quantitative analysis. However, the lag phase in nonagitated solutions containing carefully defibrillated Aβ and no fibrillar seed tended to be uncontrollably long and last at least for several days, whereas in the agitated solutions duration of lag-phase was only 3-10 minutes. It can be even speculated that under ideally quiescent conditions the fibrillation of completely defibrillated peptide would be infinitely slow. The lag period tended to decrease with increasing temperatures and showed almost no dependence on the peptide concentration. The latter observation is in sharp contrast with the classical nucleation model predicting very sharp decrease in lag period duration with increasing peptide concentrations [105].It can be speculated that in our experiments the fibrillation process is triggered on the quartz cell surface and agitation multiplies the seeds by disrupting them from the surface. It should be noted that fibrils are linear and therefore in order to observe a sharp increase in the fibrillation after the lag-period the "seeds" should be multiplied by some mechanism.

The rate of fibrillation was also constant in a wide pH range. Since there is no groups in the peptide that can loose or bind protons in the pH range 7-9 this result mainly shows the reproducibility of the process. Decrease in the fibrillation rate at lower pH results most probably from histidine protonization. The local environment of histidines changes considerably during aggregation as shown by upfield shifts of the histidine 2H NMR signals [106]. They suggested that the side chains of the aspartic acid or glutamic acid residues bond with the protonated histidines to form intramolecular salt-bridges that are important for stabilizing aggregates. However, the lower aggregation rate at lower pH where the histidines are protonated show that they likely do not form salt bridges with aspartic acid residues in fibrils.

The effect of temperature on the fibrillation rate was characterized by $\Delta H$=12 kcal/mole. This value is in the same range with $\Delta H$ values determined for $A\beta_{40}$ aggregation at acidic pH[107] and high peptide concentration. The large value shows clearly that fibrillation rate is not controlled by diffusion. Earlier it has been suggested that the sharp temperature dependence of fibrillation rate suggest involvement of hydrophobic interactions in the process, however, the theoretical background of this suggestion remains unclear. Since incubation of $A\beta_{40}$ at higher temperatures results in reversible beta-sheet accumulation [108], the $\Delta H$ can reflect the shift of equilibrium in solution towards aggregation-competent peptide conformation

In principal our experimental setup for continuous ThT-based monitoring of the fast fibrillation process of $A\beta_{42}$ in agitated solutions can be used for screening the effects of putative fibrillation inhibitors. A similar method using an artificial Aβ derivative has been proposed recently [109], but the use of native peptide may have some advantages. Nevertheless, in this case the fibrillation should be carried out in multiple-well plates.

***Impact of Zn(II) and Cu(II) on Aβ aggregation***

The study of the aggregation of $A\beta_{42}$ in the presence of Zn(II), Cu(II), and metal chelating agents has elucidated several new aspects about the influence of metal ions on the Aβ fibrillation *in vitro*.

Both Zn(II) and Cu(II) exhibited a pronounced inhibitory effect on $A\beta_{42}$ fibrillation. The concentration-dependent inhibitory effect of Zn(II) ($IC_{50}$=1.79 μM) was three times stronger than that of Cu(II) ($IC_{50}$=4.9 μM). This is in contrast to their relative binding affinities towards the $A\beta_{42}$ monomer, which is 75-fold higher for Cu(II) [62]. However, we have observed earlier that the affinity of Zn(II) towards Aβ is enhanced more than tenfold (reaching to ~ 1 μM) during partial aggregation of $A\beta_{40}$ [62], which can explain the appearance of the inhibitory effect of Zn(II) at low metal ion concentrations. Both metal ions induced fast formation of insoluble $A\beta_{42}$ aggregates, which contained stoichiometric amounts of metal ions. The inhibitory effect of metal ions is caused by the decrease of the concentration of free soluble $A\beta_{42}$, necessary for the growth of fibrils. In the case of Zn(II) Aβ aggregates are formed and the concentration of soluble Aβ decreases. In the case of Cu(II) the effect is explainable by an assumption that the Cu(II)-Aβ complex cannot join the fibrils

Metal-induced aggregation of Aβ peptides occurs most probably according to a conformational change induced aggregation mechanism as suggested earlier [110]. Zn(II)-induced aggregation of Aβ is very fast [111, 112], and therefore it is reasonable to suggests that metal complexes of Aβ may aggregate due to fast-forming hydrophobic interactions.

The suppression of $A\beta_{42}$ fibrillation by metal ions was confirmed by TEM. However, after prolonged incubation (1 week) amyloid fibrils were also detected in the samples of metal-induced $A\beta_{42}$ aggregates. Thus, fibrillation of $A\beta_{42}$ also occurs in the presence of

.

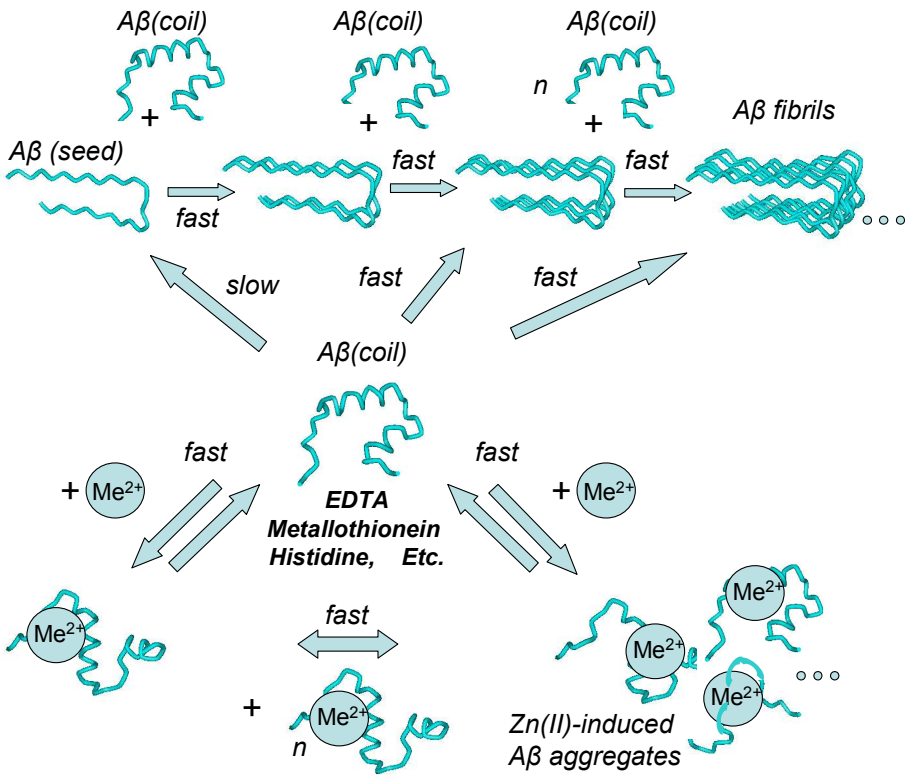


**Figure 18.** Mechanisms for assembly and fibrillogenesis of $A\beta_{42}$ peptide in the presence of Zn(II) or Cu(II) ions. $A\beta_{42}$ monomer can bind metal ion or align with preformed fibrillar seeds. Ends of the growing fibrils serve as templates for monomer addition seeds, whereas the origin of the primary seeds is unknown. The number of fibril ends acting as seeds can be increased by fragmentation of linear fibrils in agitated solution. Zn(II)-Aβ monomer formation affects the peptide conformation making it insoluble and they collapse into non-fibrillar aggregates putatively due to hydrophobic contacts. (At peptide excess free $A\beta_{42}$ can partially coprecipitate with Zn(II)-$A\beta_{42}$ into these aggregates.) Loss of metal-free $A\beta_{42}$ from solution causes the inhibition of the fibrillation. Metal chelators can sequester Zn(II) or from the aggregates leading to dissociation of $A\beta_{42}$ monomers, which contribute to fibril growth. Metal-induced aggregates obtain fibrillar structure also without addition of chelators during prolonged incubation. It is not clear whether during this incubation the Zn(II) induced $A\beta_{42}$ aggregates can be transformed to fibrillar form through monomeric state, which is always present at low equilibrium concentration, or also directly by rearrangement of its structure. A scheme for the Cu(II) effect can be drawn by replacement of Zn(II) by Cu(II) in the Figure.

metal ions and it follows that the metal-induced $A\beta_{42}$ aggregates are not dead-end products of $A\beta_{42}$ assembly (Figure 18). These observations can partially explain the contradiction between the results in literature on the effect of metal ions on fibrillation of Aβ peptides. In the conditions where the growth of fibrils is fast (as it was in our experiments) metal ions inhibit the fibrillation by lowering the concentration of free peptide; however, under conditions where the fibrillation is slow metal ions can enhance the fibrillation by causing peptide assembly to metal-induced aggregates that can further transform to fibrils.

Metal chelators with medium and high affinity can suppress the inhibitory effect of metal ions on $A\beta_{42}$ fibrillation, and their addition to metal-induced $A\beta_{42}$ aggregates stimulated fibrillation of $A\beta_{42}$. We have recently reported that the metal-induced $A\beta_{40}$ aggregates became fully soluble when the metal ions are sequestered by adding of metal chelators [62]. In the case of $A\beta_{42}$ the dissociated peptide monomers can subsequently participate in fibrillation. Kinetic results also indicate that metal ions do not prevent fibrillation but inhibit the process by lowering the concentration of soluble monomer. A schematic model describing the effect of metal ions on the fibrillation of $A\beta_{42}$, consistent with these experimental results is presented in Figure 18.

The study of His-Ala mutants of full-length $A\beta_{42}$ demonstrated that H13 and H14 contribute to the metal-induced inhibition of Aβ fibrillation. In soluble Zn(II)-Aβ and Cu(II)-Aβ complexes all three His residues participate in metal binding [22, 61]. The current model of fibrillar Aβ, constructed on the basis of experimentally derived NMR constraints, shows that the structural unit of the Aβ protofilament consists of two juxtaposed Aβ molecules, which is replicated along the fibril axis (Figure 1 d) [67, 113, 114]. Within the Aβ molecule the residues 10-23 and 30-40 are in β conformational state and form hydrogen bonds with the adjoining juxtaposed Aβ peptide units by forming cross β amyloid core structure of the fibril (Figure 1).

It follows that in Aβ fibrils His 13 and 14 residues should adapt extended β-conformation, where their imidazole units are located on the opposite sides of the peptide backbone (Figure 1). Such an arrangement differs substantially from the conformation of this segment in metal-Aβ complexes, where all His residues coordinate a single metal ion. Thus, it is evident that metal binding hinders the adoption of β-conformation in region 10-23 which has also been suggested on the basis of molecular dynamic calculations of Cu(II)-Aβ complexes [115]. Our experimental data would directly support this idea. Although the stoichiometry in aggregates is 1:1 it does not mean that the Zn(II) ions ligands are from one Aβ molecule. Therefore it seems that the involvement of histidine residues in coordinating the Zn(II) also hinders the adoption of β-conformation.

Aggregation of Aβ peptides *in vivo* occurs in the presence of endogenous metal ions as well as various metal-chelating ligands. In an environment mimicking the putative *in vivo* conditions in the regions of zinc-enriched synapses (5 μM Zn(II), 20 μM

glutamate) Zn(II) induces rapid formation of metal-induced $A\beta_{42}$ aggregates and inhibits $A\beta_{42}$ fibrillation. Thus, glutamate cannot effectively compete with $A\beta_{42}$ for Zn(II) binding. However, the brain-specific Zn(II)-binding protein MT-3 in its apo form suppressed the formation of Zn(II)-$A\beta_{42}$ aggregates. MT-3 is released by astrocytes and it is assumed to participate in the binding and uptake of Zn(II) ions from the synaptic cleft [116, 117]. The high zinc-buffering capacity of MT-s might stabilize fluctuations in concentration of free Zn(II) and avoid Zn(II)-induced aggregation of Aβ peptides. MT-3 can also solubilize $A\beta_{42}$ from already formed metal-induced Aβ aggregates. The removal of Zn(II) ions by MT-3 induced Aβ fibrillation in our experiments. However, at low physiological Aβ concentrations, 0.11 nM in brain [118], the fibrillation of monomeric Aβ molecules is a slow and unlikely process. It is repeatedly demonstrated that introduction of $A\beta_{42}$ into brain cannot induce amyloid formation *in vivo* [119]. However, if environmental metal buffering capacity is low, metal-induced Aβ aggregates could be formed in the brain and eventually transform to Aβ fibrils. It follows that metal buffering and uptake mechanisms might play a crucial role in the formation of metal-induced Aβ aggregates and defining their fate in the brain. It is known that the levels of MT-3 are substantially (10-fold) lower in AD patient's brains as compared with normal brains [120, 121]. On the light of current results it is feasible that lower levels of MT-3 might reduce zinc buffering capacity in the areas of zinc-enriched neurons, which might promote the formation of Zn(II)-induced Aβ aggregates transform into Aβ fibrils and trigger the formation of amyloid plaques. The proposed scenario for amyloid formation is in agreement with elevated concentration of zinc and copper in the cores of pathological amyloid plaques isolated from the brains of AD patients [2, 122].

Over the last decade a new therapeutic approach, metal-chelation therapy, has been established [123]. The administration of CQ suppressed plaque formation in AD model mice [79], however, only limited success was achieved in human trials [123]. Recently it was observed that CQ promotes rather than inhibits the formation of Aβ fibrils *in vitro* and the authors have proposed a careful reconsideration of the potential of CQ-based chelation therapy [82]. The *in vitro* results of the current work show that CQ itself has no direct effect on $A\beta_{42}$ fibrillation; however, in the presence of metal ions it can partially prevent or reverse the formation of Zn(II)-induced $A\beta_{42}$ assembly, which,

however, enhanced peptide fibrillation. As discussed earlier, the metal ions apparently can inhibit or enhance the fibril formation depending on the limiting step of the process. The same holds for metal chelators that convert metal-induced Aβ aggregates to monomers, which can be cleared away or enhance fibrillation when fibrillar seeds are present. Consequently the outcome of metal-chelation therapy might vary between two opposite scenarios: firstly – prevention of the formation of metal-induced Aβ aggregation and subsequent fibrillation and secondly – solubilization of metal-induced Aβ aggregates and promotion of Aβ fibrillation and amyloid formation. Nevertheless, the effect of metal chelators including CQ at cellular and organismal level might be not limited only to its interactions with Aβ aggregates. For instance it has been suggested that the beneficial effect of CQ in animal trials may arise from ionophore properties of CQ or from CQ-induced activation of Aβ degradation [81, 124]. In agreement with this suggestions, an analog of CQ with better ionophore properties, PBT2, has given more promising results in treatment [80, 125].

# SUMMARY

Alzheimer's disease (AD) is characterized by amyloid deposits in the brain that are composed mainly from fibrillar amyloid-β (Aβ) peptides and containing elevated levels of biometals zinc and copper which are being increasingly implicated in AD pathology.
In this work the effect of Zn(II) and Cu(II) on the aggregation and fibrillation of wild-type $A\beta_{42}$ and its His to Ala mutants as well as the effect of metal chelators on the metal-induced aggregates of $A\beta_{42}$ was systematically studied. Firstly a method for the monitoring of aggregation was elaborated by introducing continuous agitation of the sample. Zn(II) and Cu(II) inhibited the formation of ThT-active fibrils of $A\beta_{42}$ in concentration-dependent manner whereas effect of metal ions was quenched by metal chelators. Both metal ions induced formation of nonfibrillar amorphous $A\beta_{42}$ aggregates, which were transformed into $A\beta_{42}$ fibrils upon prolonged incubation or by addition of metal chelators with sufficiently high metal-binding affinity. Mutation of His13 and His14 residues that participate in formation of the cross-β core in fibrils, but not His6 leaded to significant weakening of the inhibitory effect of Zn(II) and Cu(II) on fibrillation of $A\beta_{42}$.

The obtained *in vitro* results suggest that reduced metal-buffering capacity of the synaptic space might be critical for the formation of Zn(II)-induced $A\beta_{42}$ aggregates, which might spontaneously transform into amyloid fibrils. Such a mechanism might enhance the probability of AD plaque formation in the regions of zinc-enriched neurons and is in agreement with the hypothesis about the causative role of synaptic zinc in pathogenesis of AD. From the viewpoint of Aβ fibrillation, the metal-chelation therapy for AD can have in first line potential as a preventive measure.

On the basis of the current results, two manuscripts have been submitted for publication:

1. Tõugu, V., A. Karafin, K. Zovo, R.S. Chung, C. Howells, A.K. West, P. Palumaa – Zn(II) and Cu(II)-induced nonfibrillar aggregates of amyloid-β peptide are transformed to amyloid fibrils, both spontaneously and under the influence of metal chelators. *J. Neurochem, - (submitted)*
2. Karafin, A., P. Palumaa, V. Tõugu, Monitoring of amyloid-β fibrillization using an improved fluorimetric method pp. xx1-xx4. In: *Alzheimer's & Parkinson's Diseases: Advances, Concepts & New Challenges – Proceedings of 9th International Conference on AD/PD, March 11-15, 2009, Prague, Czech Republic)*, Medimond International, Bologna, Italy.*(in press*)

# KOKKUVÕTE

Alzheimeri tõbe (AD) iseloomustavaks tunnuseks on amüloidsete naastude teke ajus. Naastud koosnevad peamiselt amüloid-β peptiidist ning sisaldavad kõrgenenud kontsentratsioonis biometalle, tsinki ja vaske, mida peetakse AD patoloogias oluliseks.

Käesolevas töös uuriti Zn(II) ja Cu(II) mõju $A\beta_{42}$ peptiidi ja selle His-Ala mutantide agregatsioonile ja fibrillatsioonile. Samuti uuriti süstemaatiliselt metallkelaatorite efekti metall-indutseeritud agregaatidele. Näidati, et Zn(II) ja Cu(II) inhibeerisid kontsentratsioonist sõltuvalt amüloidi moodustamist, kusjuures metall-kelaatorid surusid metallioonide mõju maha. Mõlemad uuritud ioonid indutseerisid mittefibrillaarsete amorfsete $A\beta_{42}$ agregaatide teket, mis pikaajalisel inkubeerimisel või piisavalt tugevate kelaatorite lisamisel muutusid fibrillideks. His13 ja His14, mis osalevad cross-β struktuuri moodustamisel fibrillis, aga mitte His6 mutatsioon vähendas märkimisväärselt Zn(II) ja Cu(II) mõju $A\beta_{42}$ fibrillatsioonile. Uurimisel kasutati täiustatud ThT fluorestsentsil põhinevat meetodit fibrillatsiooni kiireks läbiviimiseks ja jälgimiseks.

Saadud *in vitro* tulemused viitavad, et vähenenud metall-puhverdamise võime sünapsides võib olla Zn(II) indutseeritud agregaatide moodustamisel kriitiline. Need agregaadid omakorda võivad spontaanselt muutuda amüloidi fibrillideks. Selline mehhanism võib suurendada naastude moodustamist tsink-ergilisi neuroneid sisaldavas alas ja on kooskõlas hüpoteesiga, et sünaptiline tsink on AD patogeneesis oluline. Aβ fibrillatsiooni vaatepunktist võib metall-kelateerimis teraapia omada potentsiaali peamiselt preventatiivse meetodina.

Olemasolevate tulemuste baasil on valminud ja saadetud avaldamiseks kaks käsikirja:

1. Tõugu, V., A. Karafin, K. Zovo, R.S. Chung, C. Howells, A.K. West, P. Palumaa – Zn(II) and Cu(II)-induced nonfibrillar aggregates of amyloid-β peptide are transformed to amyloid fibrils, both spontaneously and under the influence of metal chelators. *J. Neurochem, - (submitted)*
2. Karafin, A., P. Palumaa, V. Tõugu, Monitoring of amyloid-β fibrillization using an improved fluorimetric method pp. xx1-xx4. In: *Alzheimer's & Parkinson's Diseases: Advances, Concepts & New Challenges – Proceedings of 9th International Conference on AD/PD, March 11-15, 2009, Prague, Czech Republic)*, Medimond International, Bologna, Italy.*(in press*)

# ACKNOWLEDGEMENTS

This work was supported by the European Social Fund, Archimedes Foundation, DoRa programme and Estonian Science Foundation grant 6840.

I would like to express my sincere gratitude to my supervisors Vello Tõugu and Prof. Peep Palumaa for their support and constructive criticism during my master studies. I would also like to thank Dr. Valdek Mikli and Kairit Zovo for their help with TEM experiments and Dr. Robert Tycko for kindly providing the atomic coordinates of Aβ fibrils. I am also grateful to my coworkers in Tallinn University of Technology Institute of Gene technology Proteomics Department for their help and support.

# REFERENCES


1. Biran, Y*., et al.*, "Pharmacotherapeutic Targets in Alzheimer's Disease". *J. Cell. Mol. Med.* 2008.

2. Lovell, M. A*., et al.*, Copper, iron and zinc in Alzheimer's disease senile plaques. *J. Neurol. Sci.* 1998**, 158**, (1), 47-52.

3. Miller, L. M*., et al.*, Synchrotron-based infrared and X-ray imaging shows focalized accumulation of Cu and Zn co-localized with beta-amyloid deposits in Alzheimer's disease. *J. Struct. Biol.* 2006**, 155**, (1), 30-7.

4. Blennow, K*., et al.*, Alzheimer's disease. *Lancet* 2006**, 368**, (9533), 387-403.

5. Ferri, C. P*., et al.*, Global prevalence of dementia: a Delphi consensus study. *Lancet* 2005**, 366**, (9503), 2112-17.

6. Selkoe, D. J., Alzheimer's disease: genes, proteins, and therapy. *Physiol. Rev.* 2001**, 81**, (2), 741-66.

7. Walsh, J. S*., et al.*, Survival of Outpatients with Alzheimer-Type Dementia. *Ann. Intern. Med.* 1990**, 113**, (6), 429-34.

8. Brookmeyer, R*., et al.*, Projections of Alzheimer's disease in the United States and the public health impact of delaying disease onset. *Am. J. Public Health* 1998**, 88**, (9), 1337-42.

9. Bird, T. D., Genetic factors in Alzheimer's disease. *N. Engl. J. Med.* 2005**, 352**, (9), 862-4.

10. Mayeux, R., Epidemiology of neurodegeneration. *Annu. Rev. Neurosci.* 2003**, 26**, 81-104.

11. Itoh, T*., et al.*, An electron microscopic study on atypical presenile dementia with numerous Lewy bodies in the cerebral cortex. *Folia Psychiatry Neurol. Jpn.* 1982**, 36**, (1), 99-106.

12. Joachim, C*., et al.*, Clinically diagnosed Alzheimer's disease: autopsy results in 150 cases. *Ann. Neurol.* 1988**, 24**, (1), 50-6.

13. Miyakawa, T*., et al.*, Morphological changes of microvessels in the brain with Alzheimer's disease. *Jpn. J. Psychiatry Neurol.* 1988**, 42**, (4), 819-24.

14. Glenner, G. G., Wong, C. W., Alzheimer's disease: initial report of the purification and characterization of a novel cerebrovascular amyloid protein. *Biochem. Biophys. Res. Commun.* 1984**, 120**, 885-90.

15. Masters, C. L.*, et al.*, Amyloid Plaque Core Protein in Alzheimer-Disease and Down Syndrome. *P. Natl. Acad. Sci. USA* 1985**, 82**, (12), 4245-49.

16. LaFerla, F., Oddo, S., Alzheimer's disease: Ab, tau and synaptic dysfunction. *Trends in Molecular Medcine* 2005**, 11**, (4), 170-76.

17. Clark, C. M., Karlawish, J. H., Alzheimer disease: current concepts and emerging diagnostic and therapeutic strategies. *Ann. Intern. Med.* 2003**, 138**, (5), 400-10.

18. Walsh, D. M., Selkoe, D. J., A beta oligomers - a decade of discovery. *J. Neurochem.* 2007**, 101**, (5), 1172-84.

19. McLean, C. A.*, et al.*, Soluble pool of A beta amyloid as a determinant of severity of neurodegeneration in Alzheimer's disease. *Ann. Neurol.* 1999**, 46**, (6), 860-66.

20. Bush, A. I., Drug development based on the metals hypothesis of Alzheimer's disease. *J. Alzheimers Dis.* 2008**, 15**, (2), 223-40.

21. Tomaselli, S.*, et al.*, The alpha-to-beta Conformational Transition of Alzheimer's Abeta-(1-42) Peptide in Aqueous Media is Reversible: A Step by Step Conformational Analysis Suggests the Location of beta Conformation Seeding. *Chembiochem.* 2006**, 7**, (2), 257-67.

22. Zirah, S.*, et al.*, Structural changes of region 1-16 of the Alzheimer disease amyloid beta-peptide upon zinc binding and in vitro aging. *J.Biol.Chem.* 2006**, 281**, (4), 2151-61.

23. Hardy, J. A., Higgins, G. A., Alzheimers-Disease - the Amyloid Cascade Hypothesis. *Science* 1992**, 256**, (5054), 184-85.

24. Golde, T. E., Alzheimer disease therapy: can the amyloid cascade be halted? *J. Clin. Invest.* 2003**, 111**, (1), 11-8.

25. Suzuki, N.*, et al.*, An increased percentage of long amyloid beta protein secreted by familial amyloid beta protein precursor (beta APP717) mutants. *Science* 1994**, 264**, (5163), 1336-40.

26. Eckman, C. B.*, et al.*, A new pathogenic mutation in the APP gene (I716V) increases the relative proportion of A beta 42(43). *Hum. Mol. Genet.* 1997**, 6**, (12), 2087-9.

27. Kwok, J. B.*, et al.*, Presenilin-1 mutation L271V results in altered exon 8 splicing and Alzheimer's disease with non-cored plaques and no neuritic dystrophy. *J.Biol.Chem.* 2003**, 278**, (9), 6748-54.

28. De Strooper, B., Aph-1, Pen-2, and nicastrin with presenilin generate an active gamma-secretase complex. *Neuron* 2003**, 38**, (1), 9-12.

29. Scheuner, D.*, et al.*, Secreted amyloid beta-protein similar to that in the senile plaques of Alzheimer's disease is increased in vivo by the presenilin 1 and 2 and APP mutations linked to familial Alzheimer's disease. *Nat. Med.* 1996**, 2**, (8), 864-70.

30. Cummings, B. J.*, et al.*, Beta-amyloid deposition and other measures of neuropathology predict cognitive status in Alzheimer's disease. *Neurobiol. Aging* 1996**, 17**, (6), 921-33.

31. Wilcock, G. K., Esiri, M. M., Plaques, Tangles and Dementia - a Quantitative Study. *Journal of the Neurological Sciences* 1982**, 56**, (2-3), 343-56.

32. Prohovnik, I.*, et al.*, Dissociation of neuropathology from severity of dementia in late-onset Alzheimer disease. *Neurology* 2006**, 66**, (1), 49-55.

33. Meyer-Luehmann, M.*, et al.*, Rapid appearance and local toxicity of amyloid-beta plaques in a mouse model of Alzheimer's disease. *Nature* 2008**, 451**, (7179), 720-U5.

34. Pimplikar, S. W., Reassessing the amyloid cascade hypothesis of Alzheimer's disease. *Int. J. Biochem. Cell Biol.* 2008.

35. Gong, Y.*, et al.*, Alzheimer's disease-affected brain: presence of oligomeric A beta ligands (ADDLs) suggests a molecular basis for reversible memory loss. *Proc. Natl. Acad. Sci. U S A* 2003**, 100**, (18), 10417-22.

36. Dahlgren, K. N.*, et al.*, Oligomeric and fibrillar species of amyloid-beta peptides differentially affect neuronal viability. *J.Biol.Chem.* 2002**, 277**, (35), 32046-53.

37. Martins, I. C.*, et al.*, Lipids revert inert Abeta amyloid fibrils to neurotoxic protofibrils that affect learning in mice. *EMBO J.* 2008**, 27**, (1), 224-33.

38. Resende, R.*, et al.*, Neurotoxic effect of oligomeric and fibrillar species of amyloid-beta peptide 1-42: Involvement of endoplasmic reticulum calcium release in oligomer-induced cell death. *Neuroscience* 2008.

39. Cerpa, W.*, et al.*, Is there a role for copper in neurodegenerative diseases? *Mol. Aspects. Med.* 2005**, 26**, (4-5), 405-20.

40. Kardos, J.*, et al.*, Nerve endings from rat brain tissue release copper upon depolarization. A possible role in regulating neuronal excitability. *Neurosci. Lett.* 1989**, 103**, (2), 139-44.

41. Hartter, D. E., Barnea, A., Evidence for Release of Copper in the Brain - Depolarization-Induced Release of Newly Taken-up Copper-67. *Synapse* 1988**, 2**, (4), 412-15.

42. Hopt, A.*, et al.*, Methods for studying synaptosomal copper release. *J. Neurosci. Methods* 2003**, 128**, (1-2), 159-72.

43. Vasto, S.*, et al.*, Inflammation, genes and zinc in Alzheimer's disease. *Brain. Res. Rev.* 2008**, 58**, (1), 96-105.

44. Assaf, S. Y., Chung, S. H., Release of endogenous Zn2+ from brain tissue during activity. *Nature* 1984**, 308**, (5961), 734-6.

45. Howell, G. A.*, et al.*, Stimulation-induced uptake and release of zinc in hippocampal slices. *Nature* 1984**, 308**, (5961), 736-8.

46. Adlard, P. A., Bush, A. I., Metals and Alzheimer's disease. *J. Alzheimers Dis.* 2006**, 10**, (2-3), 145-63.

47. Konoha, K.*, et al.*, Zinc neurotoxicity and its role in neurodegenerative diseases. *J. Health Sci.* 2006**, 52**, (1), 1-8.

48. Bush, A. I., Tanzi, R. E., Therapeutics for Alzheimer's disease based on the metal hypothesis. *Neurotherapeutics* 2008**, 5**, (3), 421-32.

49. Dong, J.*, et al.*, Metal binding and oxidation of amyloid-beta within isolated senile plaque cores: Raman microscopic evidence. *Biochemistry* 2003**, 42**, (10), 2768-73.

50. Huang, X.*, et al.*, Cu(II) potentiation of alzheimer abeta neurotoxicity. Correlation with cell-free hydrogen peroxide production and metal reduction. *J.Biol.Chem.* 1999**, 274**, (52), 37111-6.

51. Meloni, G.*, et al.*, Metal swap between Zn7-metallothionein-3 and amyloid-beta-Cu protects against amyloid-beta toxicity. *Nat. Chem. Biol.* 2008**, 4**, (6), 366-72.

52. Lee, J. Y.*, et al.*, Contribution by synaptic zinc to the gender-disparate plaque formation in human Swedish mutant APP transgenic mice. *Proc. Natl. Acad. Sci. U S A* 2002**, 99**, (11), 7705-10.

53. Sparks, D. L., Schreurs, B. G., Trace amounts of copper in water induce beta-amyloid plaques and learning deficits in a rabbit model of Alzheimer's disease. *Proc. Natl. Acad. Sci. U S A* 2003**, 100**, (19), 11065-9.

54. Bayer, T. A.*, et al.*, Dietary Cu stabilizes brain superoxide dismutase 1 activity and reduces amyloid Abeta production in APP23 transgenic mice. *Proc. Natl. Acad. Sci. U S A* 2003**, 100**, (24), 14187-92.

55. Karr, J. W.*, et al.*, N-Terminal deletions modify the Cu2+ binding site in amyloid-beta. *Biochemistry* 2005**, 44**, (14), 5478-87.

56. Jiang, D.*, et al.*, Redox Reactions of Copper Complexes Formed with Different beta-Amyloid Peptides and Their Neuropathalogical Relevance. *Biochemistry* 2007**, 46**, (32), 9270-82.

57. Ali, F. E.*, et al.*, Copper and zinc mediated oligomerisation of A beta peptides. *Int. J. Pept. Res. Ther.* 2006**, 12**, (2), 153-64.

58. Clements, A.*, et al.*, Aggregation and metal-binding properties of mutant forms of the amyloid A beta peptide of Alzheimer's disease. *J. Neurochem.* 1996**, 66**, (2), 740-7.

59. Atwood, C. S.*, et al.*, Characterization of copper interactions with alzheimer amyloid beta peptides: identification of an attomolar-affinity copper binding site on amyloid beta1-42. *J. Neurochem.* 2000**, 75**, (3), 1219-33.

60. Miura, T.*, et al.*, Metal binding modes of Alzheimer's amyloid beta-peptide in insoluble aggregates and soluble complexes. *Biochemistry* 2000**, 39**, (23), 7024-31.

61. Syme, C. D., Viles, J. H., Solution (1)H NMR investigation of Zn(2+) and Cd(2+) binding to amyloid-beta peptide (Abeta) of Alzheimer's disease. *Biochim. Biophys. Acta* 2006**, 1764**, (2), 246-56.

62. Tougu, V.*, et al.*, Binding of zinc(II) and copper(II) to the full-length Alzheimer's amyloid-beta peptide. *J. Neurochem.* 2008**, 104**, (5), 1249-59.

63. Masuoka, J., Saltman, P., Zinc(II) and copper(II) binding to serum albumin. A comparative study of dog, bovine, and human albumin. *J.Biol.Chem.* 1994**, 269**, (41), 25557-61.

64. Faller, P., Hureau, C., Bioinorganic chemistry of copper and zinc ions coordinated to amyloid-beta peptide. *Dalton Trans.* 2009, (7), 1080-94.

65. Harrison, R. S.*, et al.*, Amyloid peptides and proteins in review. *Rev. Physiol. Biochem. Pharmacol.* 2007**, 159**, 1-77.

66. O'Nuallain, B.*, et al.*, Thermodynamics of abeta(1-40) amyloid fibril elongation. *Biochemistry* 2005**, 44**, (38), 12709-18.

67. Petkova, A. T.*, et al.*, Experimental Constraints on Quaternary Structure in Alzheimer's beta-Amyloid Fibrils. *Biochemistry* 2006**, 45**, (2), 498-512.

68. Tycko, R., Insights into the amyloid folding problem from solid-state NMR. *Biochemistry* 2003**, 42**, (11), 3151-9.

69. Paravastua, A. K.*, et al.*, Molecular structural basis for polymorphism in Alzheimer's beta-amyloid fibrils. *P. Natl. Acad. Sci. USA* 2008**, 105**, (47), 18349-54.

70. Bush, A. I.*, et al.*, Rapid induction of Alzheimer A beta amyloid formation by zinc. *Science* 1994**, 265**, (5177), 1464-7.

71. Esler, W. P.*, et al.*, Zinc-induced aggregation of human and rat beta-amyloid peptides in vitro. *J. Neurochem.* 1996**, 66**, (2), 723-32.

72. Cherny, R. A.*, et al.*, Aqueous dissolution of Alzheimer's disease Abeta amyloid deposits by biometal depletion. *J.Biol.Chem.* 1999**, 274**, (33), 23223-8.

73. Yoshiike, Y.*, et al.*, New insights on how metals disrupt amyloid beta-aggregation and their effects on amyloid-beta cytotoxicity. *J.Biol.Chem.* 2001**, 276**, (34), 32293-9.

74. Raman, B.*, et al.*, Metal Ion-dependent Effects of Clioquinol on the Fibril Growth of an Amyloid {beta} Peptide. *J.Biol.Chem.* 2005**, 280**, (16), 16157-62.

75. Ha, C.*, et al.*, Metal Ions Differentially Influence the Aggregation and Deposition of Alzheimer's beta-Amyloid on a Solid Template. *Biochemistry* 2007**, 46**, (20), 6118-25.

76. Klug, G. M.*, et al.*, Beta-amyloid protein oligomers induced by metal ions and acid pH are distinct from those generated by slow spontaneous ageing at neutral pH. *Eur. J. Biochem.* 2003**, 270**, (21), 4282-93.

77. Ricchelli, F.*, et al.*, Aluminum-triggered structural modifications and aggregation of beta-amyloids. *Cell. Mol. Life Sci.* 2005**, 62**, (15), 1724-33.

78. Huang, J.*, et al.*, The solution structure of rat Abeta-(1-28) and its interaction with zinc ion: insights into the scarcity of amyloid deposition in aged rat brain. *J. Biol. Inorg. Chem.* 2004**, 9**, (5), 627-35.

79. Cherny, R. A.*, et al.*, Treatment with a copper-zinc chelator markedly and rapidly inhibits beta-amyloid accumulation in Alzheimer's disease transgenic mice. *Neuron* 2001**, 30**, (3), 665-76.

80. Adlard, P. A.*, et al.*, Rapid restoration of cognition in Alzheimer's transgenic mice with 8-hydroxy quinoline analogs is associated with decreased interstitial Abeta. *Neuron* 2008**, 59**, (1), 43-55.

81. White, A. R.*, et al.*, Degradation of the Alzheimer disease amyloid beta-peptide by metal-dependent up-regulation of metalloprotease activity. *J.Biol.Chem.* 2006**, 281**, (26), 17670-80.

82. Bolognin, S.*, et al.*, Mutual Stimulation of Beta-Amyloid Fibrillogenesis by Clioquinol and Divalent Metals. *Neuromol. Med.* 2008.

83. Jarrett, J. T., Lansbury, P. T., Jr., Amyloid fibril formation requires a chemically discriminating nucleation event: studies of an amyloidogenic sequence from the bacterial protein OsmB. *Biochemistry* 1992**, 31**, (49), 12345-52.

84. Kusumoto, Y.*, et al.*, Temperature dependence of amyloid beta-protein fibrillization. *Proc. Natl. Acad. Sci. U S A* 1998**, 95**, (21), 12277-82.

85. Brown, A. M.*, et al.*, Selective aggregation of endogenous beta-amyloid peptide and soluble amyloid precursor protein in cerebrospinal fluid by zinc. *J. Neurochem.* 1997**, 69**, (3), 1204-12.

86. Ma, J.*, et al.*, Amyloid-associated proteins alpha 1-antichymotrypsin and apolipoprotein E promote assembly of Alzheimer beta-protein into filaments. *Nature* 1994**, 372**, (6501), 92-4.

87. Dzwolak, W., Pecul, M., Chiral bias of amyloid fibrils revealed by the twisted conformation of Thioflavin T: An induced circular dichroism/DFT study. *FEBS Lett.* 2005**, 579**, (29), 6601-3.

88. Stsiapura, V. I., *et al.*, Computational Study of Thioflavin T Torsional Relaxation in the Excited State. *The Journal of Physical Chemistry A* 2007**, 111**, (22), 4829-35.

89. Levine, H., Thioflavine-T Interaction with Amyloid Beta-Sheet Structures. *Amyloid-Int. J. Exp. Clin. Investig.* 1995**, 2**, (1), 1-6.

90. Smith, D. P., *et al.*, Concentration Dependent Cu(2+) Induced Aggregation and Dityrosine Formation of the Alzheimer's Disease Amyloid-beta Peptide. *Biochemistry* 2007.

91. Isaacs, A. M., *et al.*, Acceleration of amyloid beta -peptide aggregation by physiological concentrations of calcium. *J.Biol.Chem.* 2006.

92. Siegel, S. J., *et al.*, The oxidative stress metabolite 4-hydroxynonenal promotes Alzheimer protofibril formation. *Biochemistry* 2007**, 46**, (6), 1503-10.

93. Bourhim, M., *et al.*, Linear quantitation of Abeta aggregation using Thioflavin T: Reduction in fibril formation by colostrinin. *J. Neurosci. Methods* 2007**, 160**, (2), 264-8.

94. Lee, S., *et al.*, Role of aggregation conditions in structure, stability, and toxicity of intermediates in the Abeta fibril formation pathway. *Protein Sci.* 2007**, 16**, (4), 723-32.

95. Nielsen, L., *et al.*, Effect of environmental factors on the kinetics of insulin fibril formation: elucidation of the molecular mechanism. *Biochemistry* 2001**, 40**, (20), 6036-46.

96. Eriste, E., *et al.*, Purification of recombinant human apometallothionein-3 and reconstitution with zinc. *Protein Expr. Purif.* 2003**, 31**, (1), 161-5.

97. Stine, W. B., Jr., *et al.*, In vitro characterization of conditions for amyloid-beta peptide oligomerization and fibrillogenesis. *J.Biol.Chem.* 2003**, 278**, (13), 11612-22.

98. J.H.R.Kägi, Evolution, structure and chemical activity of class I metallothioneins: an overview. In *Methallothionein III: Biological roles and medical implications*, Eds. K.T.Suzuki, N. I., M.Kimura; Birkhäuser: Basel; Boston; Berlin, 1993; pp 29-56.

99. R.M.C.Dawson, D. C. E., W.H.Elliott, K.M.Jones, *Data for Biochemical Research*. Oxford University Press: Oxford, 1986; p 544.

100. Garzon-Rodriguez, W., *et al.*, Binding of Zn(II), Cu(II), and Fe(II) ions to Alzheimer's A beta peptide studied by fluorescence. *Bioorg. Med. Chem. Lett.* 1999**, 9**, (15), 2243-8.

101. Syme, C. D., *et al.*, Copper binding to the amyloid-beta (Abeta) peptide associated with Alzheimer's disease: folding, coordination geometry, pH dependence, stoichiometry, and affinity of Abeta-(1-28): insights from a range of complementary spectroscopic techniques. *J.Biol.Chem.* 2004**, 279**, (18), 18169-77.

102. Bitan, G., *et al.*, Amyloid beta -protein (Abeta) assembly: Abeta 40 and Abeta 42 oligomerize through distinct pathways. *Proc. Natl. Acad. Sci. U S A* 2003**, 100**, (1), 330-5.

103. Kelly, J. W., Mechanisms of amyloidogenesis. *Nat. Struct. Biol.* 2000**, 7**, (10), 824-6.

104. Serio, T. R., *et al.*, Nucleated conformational conversion and the replication of conformational information by a prion determinant. *Science* 2000**, 289**, (5483), 1317-21.

105. Jarrett, J. T., Lansbury, P. T., Jr., Seeding "one-dimensional crystallization" of amyloid: a pathogenic mechanism in Alzheimer's disease and scrapie? *Cell* 1993**, 73**, (6), 1055-8.

106. Hou, L., *et al.*, Solution NMR studies of the A beta(1-40) and A beta(1-42) peptides establish that the Met35 oxidation state affects the mechanism of amyloid formation. *J. Am. Chem. Soc.* 2004**, 126**, (7), 1992-2005.

107. Massi, F., Straub, J. E., Energy landscape theory for Alzheimer's amyloid beta-peptide fibril elongation. *Proteins* 2001**, 42**, (2), 217-29.

108. Gursky, O., Aleshkov, S., Temperature-dependent beta-sheet formation in beta-amyloid Abeta(1-40) peptide in water: uncoupling beta-structure folding from aggregation. *Biochim. Biophys. Acta* 2000**, 1476**, (1), 93-102.

109. Dolphin, G. T., *et al.*, Designed Amyloid beta Peptide Fibril-A Tool for High-Throughput Screening of Fibril Inhibitors. *ChemMedChem* 2007**, 2**, (11), 1613-23.

110. Talmard, C., *et al.*, Amyloid-Beta Peptide Forms Monomeric Complexes With Cu(II) and Zn(II) Prior to Aggregation. *Chembiochem.* 2007**, 8**, (2), 163-65.

111. Huang, T. H., *et al.*, Fibrillogenesis of Alzheimer Abeta peptides studied by fluorescence energy transfer. *J. Mol. Biol.* 1997**, 269**, (2), 214-24.

112. Noy, D., *et al.*, Zinc-amyloid beta interactions on a millisecond time-scale stabilize non-fibrillar Alzheimer-related species. *J. Am. Chem. Soc.* 2008**, 130**, (4), 1376-83.

113. Luhrs, T., *et al.*, 3D structure of Alzheimer's amyloid-beta(1-42) fibrils. *Proc. Natl. Acad. Sci. U S A* 2005**, 102**, (48), 17342-7.

114. Nelson, R., *et al.*, Structure of the cross-beta spine of amyloid-like fibrils. *Nature* 2005**, 435**, (7043), 773-8.

115. Jiao, Y., Yang, P., Mechanism of Copper(II) Inhibiting Alzheimer's Amyloid beta-Peptide from Aggregation: A Molecular Dynamics Investigation. *J. Phys. Chem. B* 2007.

116. Uchida, Y., *et al.*, Growth inhibitory factor prevents neurite extension and the death of cortical neurons caused by high oxygen exposure through hydroxyl radical scavenging. *J.Biol.Chem.* 2002**, 277**, (35), 32353-9.

117. Barnham, K. J., Bush, A. I., Metals in Alzheimer's and Parkinson's diseases. *Curr. Opin. Chem. Biol.* 2008**, 12**, (2), 222-8.

118. Sjogren, M., *et al.*, Tau and Abeta42 in cerebrospinal fluid from healthy adults 21-93 years of age: establishment of reference values. *Clin. Chem.* 2001**, 47**, (10), 1776-81.

119. Meyer-Luehmann, M., *et al.*, Exogenous induction of cerebral beta-amyloidogenesis is governed by agent and host. *Science* 2006**, 313**, (5794), 1781-4.

120. Tsuji, S., *et al.*, Molecular cloning of human growth inhibitory factor cDNA and its down-regulation in Alzheimer's disease. *EMBO J.* 1992**, 11**, (13), 4843-50.

121. Yu, W. H., *et al.*, Metallothionein III is reduced in Alzheimer's disease. *Brain Res.* 2001**, 894**, (1), 37-45.

122. Hutchinson, R. W., *et al.*, Imaging and spatial distribution of beta-amyloid peptide and metal ions in Alzheimer's plaques by laser ablation-inductively coupled plasma-mass spectrometry. *Anal.Biochem.* 2005**, 346**, (2), 225-33.

123. Ritchie, C. W., *et al.*, Metal-protein attenuation with iodochlorhydroxyquin (clioquinol) targeting Abeta amyloid deposition and toxicity in Alzheimer disease: a pilot phase 2 clinical trial. *Arch. Neurol.* 2003**, 60**, (12), 1685-91.

124. Crouch, P. J., *et al.*, Restored degradation of the Alzheimer's amyloid-beta peptide by targeting amyloid formation. *J. Neurochem.* 2009**, 108**, 1198-207.

125. Lannfelt, L., *et al.*, Safety, efficacy, and biomarker findings of PBT2 in targeting Abeta as a modifying therapy for Alzheimer's disease: a phase IIa, double-blind, randomised, placebo-controlled trial. *Lancet Neurol.* 2008**, 7**, (9), 779-86.